FOR UNRESTRICTED DISTRIBUTION
DATE ______________________ WEC

Westinghouse Energy Systems

WCAP-12354

WESTINGHOUSE CLASS 3

ANALYSIS OF CAPSULE X FROM THE DUKE POWER COMPANY MCGUIRE UNIT 1 REACTOR VESSEL RADIATION SURVEILLANCE PROGRAM

S. E. Yanichko

S. L. Anderson

L. Albertin

N. K. Ray

August 1989

Work performed under Shop Order No. DSMJ-106

APPROVED: T. A. Meyer

T. A. Meyer, Manager

Structural Materials and Reliability Technology

Prepared by Westinghouse for the Duke Power Company

10

WESTINGHOUSE ELECTRIC CORPORATION
Energy Systems Division
P.O. Box 2728
Pittsburgh, Pennsylvania 15230

PREFACE

This report has been technically reviewed and verified.

	Reviewer	
Sections 1 through 5 and 7, 8	E. Terek	E. Terek
Section 6	E. P. Lippincott	E. P. Lippincott

TABLE OF CONTENTS

LIST OF ILLUSTRATIONS

LIST OF ILLUSTRATIONS (Cont)

LIST OF TABLES

LIST OF TABLES (Cont)

LIST OF TABLES (Cont)

SECTION 1
SUMMARY OF RESULTS

The analysis of the reactor vessel material contained in Capsule X, the second surveillance capsule to be removed from the Duke Power Company McGuire Unit 1 reactor pressure vessel, led to the following conclusions:

- o The capsule received an average fast neutron fluence (E > 1.0 MeV) of 1.38×10^{19} n/cm^2.

- o Irradiation of the reactor vessel intermediate shell Plate B5012-1, to 1.38×10^{19} n/cm, resulted in 30 and 50 ft-lb transition temperature increases of 65 and 55°F respectively, for specimens oriented normal to the major working direction (transverse orientation) and 45°F for specimens oriented parallel to the major working direction (longitudinal orientation).

- o Weld metal irradiated to 1.38×10^{19} n/cm^2 resulted in a 165 and 185°F increase in the 30 and 50 ft-lb transition temperature respectively.

- o Irradiation to 1.38×10^{19} n/cm^2 resulted in no decrease in the average upper shelf energy of Plate B5012-1 (transverse orientation) and an upper shelf energy decrease of 29 ft-lbs for the weld metal. Both materials exhibit a more than adequate shelf level for continued safe plant operation.

- o Comparison of the 30 ft-lb transition temperature increases for the McGuire Unit 1 surveillance material with predicted increases using the methods of NRC Regulatory Guide 1.99, Revision 2, shows that the Plate B5012-1 material transition temperature increase was 4°F greater than predicted. This increase is bounded by the 2 sigma allowance for shift prediction of 34°F. The weld metal showed a transition temperature increase that was 64°F less than the prediction.

Impact Of Test Results On Plant Life Extension

- The measured ΔRT_{NDT} values are significantly lower than those values predicted at 1.38×10^{19} n/cm^2 (~22 EFPY) for the axial welds. This can provide for less restrictive ASME, Section III, Appendix G heatup and cooldown curves for future plant life. The future surveillance capsule's test data will be required to determine what potential benefit, if any, may be utilized for heatup and cooldown curves developed for an extended vessel life, i.e. Plant Life Extension.

- PTS margin should exist for some amount of life extension beyond the current license life of the McGuire Unit 1 based on the predicted values of RT_{PTS}. The data reported here can imply additional PTS margin since the measured RT_{NDT} values for the axial weld material are significantly less than the predicted values using Regulatory Guide 1.99, Revision 2 prediction methods. However, this benefit cannot be readily obtained since the PTS rule requires the use of only predicted RT_{NDT} (i.e. RT_{PTS}) values.

SECTION 2
INTRODUCTION

This report presents the results of the examination of Capsule X, the second capsule to be removed from the reactor in the continuing surveillance program which monitors the effects of neutron irradiation on the Duke Power Company McGuire Unit 1 reactor pressure vessel materials under actual operating conditions.

The surveillance program for the Duke Power Company McGuire Unit 1 reactor pressure vessel materials was designed and recommended by the Westinghouse Electric Corporation. A description of the surveillance program and the preirradiation mechanical properties of the reactor vessel materials are presented by Davidson and Yanichko.[1] The surveillance program was planned to cover the 40-year design life of the reactor pressure vessel and was based on ASTM E-185-73, "Recommended Practice for Surveillance Tests for Nuclear Reactor Vessels". Westinghouse Energy Systems personnel were contracted to aid in the preparation of procedures for removing the capsule from the reactor and its shipment to the Westinghouse Research and Development Laboratory, where the postirradiation mechanical testing of the Charpy V-notch impact and tensile surveillance specimens was performed.

This report summarizes testing and the postirradiation data obtained from surveillance Capsule X removed from the Duke Power Company McGuire Unit 1 reactor vessel and discusses the analysis of the data. The data are also compared to capsule U[2] which was removed from the reactor in 1984.

SECTION 3
BACKGROUND

The ability of the large steel pressure vessel containing the reactor core and its primary coolant to resist fracture constitutes an important factor in ensuring safety in the nuclear industry. The beltline region of the reactor pressure vessel is the most critical region of the vessel because it is subjected to significant fast neutron bombardment. The overall effects of fast neutron irradiation on the mechanical properties of low alloy ferritic pressure vessel steels such as SA533 Grade B Class 1 (base material of the McGuire Unit 1 reactor pressure vessel beltline) are well documented in the literature. Generally, low alloy ferritic materials show an increase in hardness and tensile properties and a decrease in ductility and toughness under certain conditions of irradiation.

A method for performing analyses to guard against fast fracture in reactor pressure vessels has been presented in "Protection Against Non-ductile Failure," Appendix G to Section III of the ASME Boiler and Pressure Vessel Code. The method utilizes fracture mechanics concepts and is based on the reference nil-ductility temperature (RT_{NDT}).

RT_{NDT} is defined as the greater of either the drop weight nil-ductility transition temperature (NDTT per ASTM E-208) or the temperature 60°F less than the 50 ft lb (and 35-mil lateral expansion) temperature as determined from Charpy specimens oriented normal (transverse) to the major working direction of the material. The RT_{NDT} of a given material is used to index that material to a reference stress intensity factor curve (K_{IR} curve) which appears in Appendix G of the ASME Code. The K_{IR} curve is a lower bound of dynamic, crack arrest, and static fracture toughness results obtained from several heats of pressure vessel steel. When a given material is indexed to the K_{IR} curve, allowable stress intensity factors can be obtained for this material as a function of temperature. Allowable operating limits can then be determined utilizing these allowable stress intensity factors.

RT_{NDT} and, in turn, the operating limits of nuclear power plants can be adjusted to account for the effects of radiation on the reactor vessel material properties. The radiation embrittlement or changes in mechanical properties of a given reactor pressure vessel steel can be monitored by a reactor surveillance program such as the McGuire Unit 1 Reactor Vessel Radiation Surveillance Program,[1] in which a surveillance capsule is periodically removed from the operating nuclear reactor and the encapsulated specimens are tested. The increase in the average Charpy V-notch 30 ft lb temperature (ΔRT_{NDT}) due to irradiation is added to the original RT_{NDT} to adjust the RT_{NDT} for radiation embrittlement. This adjusted RT_{NDT} (RT_{NDT} initial + ΔRT_{NDT}) is used to index the material to the K_{IR} curve and, in turn, to set operating limits for the nuclear power plant which take into account the effects of irradiation on the reactor vessel materials.

SECTION 4
DESCRIPTION OF PROGRAM

Six surveillance capsules for monitoring the effects of neutron exposure on the McGuire Unit 1 reactor pressure vessel core region material were inserted in the reactor vessel prior to initial plant startup. The capsules were positioned in the reactor vessel between the neutron shield pads and the vessel wall at locations shown in Figure 4-1. The vertical center of the capsules is opposite the vertical center of the core.

Capsule X (Figure 4-2) was removed after 4.33 effective full power years of plant operation. This capsule contained Charpy V-notch impact, tensile, and 1/2T - Compact Tension fracture mechanics specimens from the reactor vessel intermediate shell Plate B5012-1, submerged arc weld metal representative of the beltline region intermediate shell longitudinal weld seams and Charpy V-notch specimens from weld heat-affected zone (HAZ) material. All heat-affected zone specimens were obtained from within the HAZ of Plate B5012-1 of the representative weld.

The chemistry and heat treatment of the surveillance material are presented in Table 4-1 and Table 4-2, respectively. The chemical analyses reported in table 4-1 were obtained from unirradiated material used in the surveillance program. In addition, a chemical analysis was performed on irradiated Charpy specimens from the intermediate shell Plate B5012-1 and weld metal and is reported in Table 4-1.

All test specimens were machined from the 1/4 thickness location of the plate. Test specimens represent material taken at least one plate thickness from the quenched end of the plate. All base metal Charpy V-notch impact and tensile specimens were oriented with the longitudinal axis of the specimen both normal to (transverse orientation) and parallel to (longitudinal orientation) the principal working direction of the plate. Charpy V-notch specimens from the weld metal were oriented with the longitudinal axis of the specimens transverse to the weld direction. Tensile specimens were oriented with the longitudinal axis of the specimens normal to the welding direction. The 1/2T Compact Tension (CT) test specimens in Capsule X were machined such that the simulated crack in the specimen would propagate normal and parallel to the major working direction for the plate specimens and parallel to the weld direction for weld specimens. All specimens were fatigue precracked per ASTM E399-70T.

Capsule X contained dosimeter wires of pure iron, copper, nickel, and unshielded aluminum-cobalt. In addition, cadmium-shielded dosimeters of Neptunium (Np^{237}) and Uranium (U^{238}) were contained in the capsule.

Thermal monitors made from two low-melting eutectic alloys and sealed in Pyrex tubes were included in the capsule and were located as shown in Figure 4-2. The two eutectic alloys and their melting points are:

2.5% Ag, 97.5% Pb	Melting Point 579°F (304°C)
1.75% Ag, 0.75% Sn, 97.5% Pb	Melting Point 590°F (310°C)

The arrangement of the various mechanical test specimens, dosimeters and thermal monitors contained in Capsule X are shown in Figure 4-2.

TABLE 4-1

CHEMICAL COMPOSITION OF
THE MCGUIRE UNIT 1 REACTOR VESSEL
SURVEILLANCE MATERIALS

Element	Plate B5012-1 (Wt. %)		Weld Metal[a] (Wt. %)		
C	0.21	-	0.10	-	
S	0.016	-	0.008	-	
N_2	0.003	-	0.008	-	
Co	0.016	-	0.014	-	
Cu	0.087	-	0.21	0.20	b
Si	0.23	-	0.24	0.23	b
Mo	0.57	-	0.55	0.54	b
Ni	0.60	-	0.88	0.91	b
Mn	1.26	-	1.36	1.19	b
Cr	0.068	-	0.04	0.05	b
V	0.003	-	0.04	-	b
P	0.010	-	0.011	0.010	b
Sn	0.007	-	0.007	-	
Ti	0.005	-	<0.010	-	
Pb	0.001	-	<0.001	-	
W	<0.001	-	<0.0100	-	
Zr	<0.003	-	<0.001	-	
As	0.008	-	0.009	-	
Cb	<0.001	-	<0.010	-	
B	<0.003	-	<0.001	-	
Sb	<0.001	-	0.002	-	

(a) Surveillance weld specimens were made of the same weld wire and flux as the intermediate shell longitudinal weld seams (Tandem Weld Wire Heats 20291 and 12008 and Linde 1092 Flux Lot 3854)

(b) Analysis performed on irradiated Charpy weld specimen DW-15 from capsule U.

TABLE 4-2

HEAT TREATMENT OF THE MCGUIRE UNIT 1
REACTOR VESSEL SURVEILLANCE MATERIALS

Material	Temperature (°F)	Time (hr)	Coolant
Intermediate Shell	1550/1650	4	Water quenched
Plate B5012-1	1200/1250	4	Air cooled
	1125/1175	40	Furnace cooled
Weld Metal	1125/1175	40	Furnace cooled

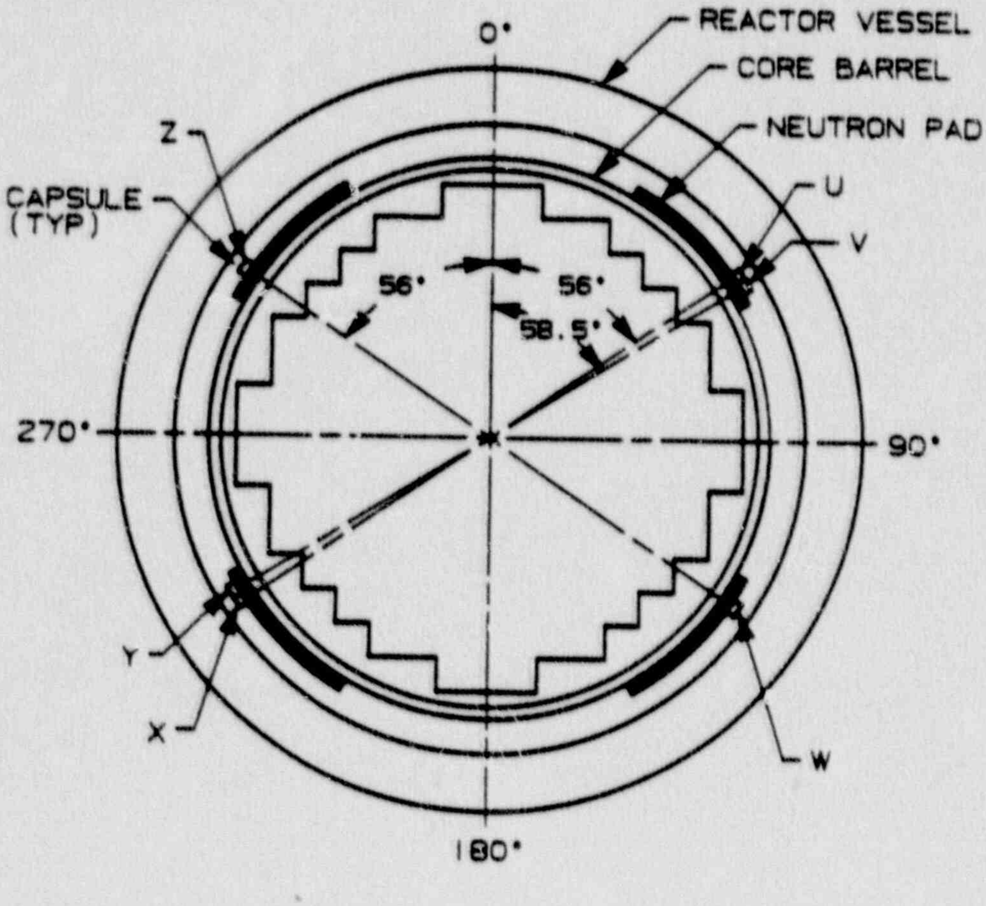

Figure 4-1. Arrangement of Surveillance Capsules in the McGuire Unit 1 Reactor Vessel

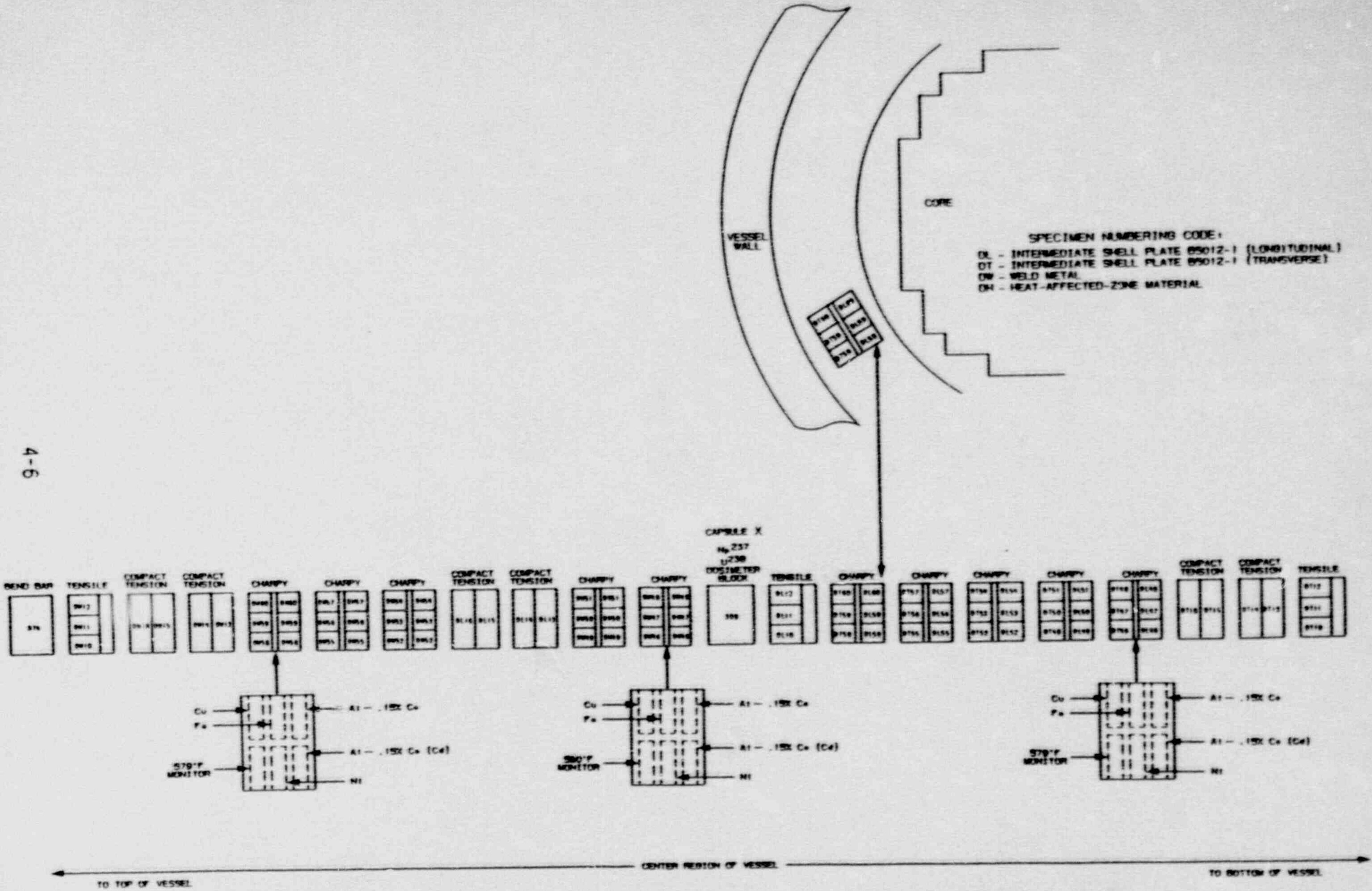

Figure 4-2 Capsule X Diagram Showing Location of Specimens, Thermal Monitors, and Dosimeters

SECTION 5
TESTING OF SPECIMENS FROM CAPSULE X

5-1. OVERVIEW

The postirradiation mechanical testing of the Charpy V-notch and tensile specimens was performed at the Westinghouse Research and Development Laboratory with consultation by Westinghouse Nuclear Energy Systems personnel. Testing was performed in accordance with 10CFR50, Appendices G and H[3], ASTM Specification E185-82 and Westinghouse Procedure MHL 8402, Revision 1 as modified by Westinghouse RMF Procedures 8102, Revision 1 and 8103, Revision 1.

Upon receipt of the capsule at the laboratory, the specimens and spacer blocks were carefully removed, inspected for identification number, and checked against the master list in WCAP-9195.[1] No discrepancies were found.

Examination of the two low-melting 304°C (579°F) and 310°C (590°F) eutectic alloys indicated no melting of either type of thermal monitor. Based on this examination, the maximum temperature to which the test specimens were exposed was less than 304°C (579°F).

The Charpy impact tests were performed per ASTM Specification E23-82 and RMF Procedure 8103, Revision 1 on a Tinius-Olsen Model 74, 358J machine. The tup (striker) of the Charpy machine is instrumented with an Effects Technology model 500 instrumentation system. With this system, load-time and energy-time signals can be recorded in addition to the standard measurement of Charpy energy (E_D). From the load-time curve, the load of general yielding (P_{GY}), the time to general yielding (t_{GY}), the maximum load (P_M), and the time to maximum load (t_M) can be determined. Under some test conditions, a sharp drop in load indicative of fast fracture was observed. The load at which fast fracture was initiated is identified as the fast fracture load (P_F), and the load at which fast fracture terminated is identified as the arrest load (P_A).

The energy at maximum load (E_M) was determined by comparing the energy-time record and the load-time record. The energy at maximum load is approximately equivalent to the energy required to initiate a crack in the specimen. Therefore, the propagation energy for the crack (E_p) is the difference between the total energy to fracture (E_D) and the energy at maximum load.

The yield stress (σy) is calculated from the three point bend formula. The flow stress is calculated from the average of the yield and maximum loads, also using the three point bend formula.

Percentage shear was determined from postfracture photographs using the ratio-of-areas methods in compliance with ASTM Specification A370-77. The lateral expansion was measured using a dial gage rig similar to that shown in the same specification.

Tension tests were performed on a 20,000-pound Instron, split-console test machine (Model 1115) per ASTM Specifications E8-83 and E21-79, and RMF Procedure 8102, Revision 1. All pull rods, grips, and pins were made of Inconel 718 hardened to Rc45. The upper pull rod was connected through a universal joint to improve axiality of loading. The tests were conducted at a constant crosshead speed of 0.05 inch per minute throughout the test.

Deflection measurements were made with a linear variable displacement transducer (LVDT) extensometer. The extensometer knife edges were spring-loaded to the specimen and operated through specimen failure. The extensometer gage length is 1.00 inch. The extensometer is rated as Class B-2 per ASTM E83-67.

Elevated test temperatures were obtained with a three-zone electric resistance split-tube furnace with a 9-inch hot zone. All tests were conducted in air.

Because of the difficulty in remotely attaching a thermocouple directly to the specimen, the following procedure was used to monitor specimen temperature. Chromel-alumel thermocouples were inserted in shallow holes in the center and each end of the gage section of a dummy specimen and in each grip. In test configuration, with a slight load on the specimen, a plot of specimen temperature versus upper and lower grip and controller temperatures was developed over the range room temperature to 550°F (288°C). The upper grip was used to control the furnace temperature. During the actual testing the grip temperatures were used to obtain desired specimen temperatures. Experiments indicated that this method is accurate to plus or minus 2°F.

The yield load, ultimate load, fracture load, total elongation, and uniform elongation were determined directly from the load-extension curve. The yield strength, ultimate strength, and fracture strength were calculated using the original cross-sectional area. The final diameter and final gage length were determined from postfracture photographs. The fracture area used to calculate the fracture stress (true stress at fracture) and percent reduction in area was computed using the final diameter measurement.

5.2. CHARPY V-NOTCH IMPACT TEST RESULTS

The results of Charpy V-notch impact tests performed on the various materials contained in Capsule X irradiated to approximately 1.38×10^{19} n/cm^2 at 550°F are presented in Tables 5-1 through 5-4 and Figures 5-1 through 5-4. The transition temperature increases and upper shelf energy decreases for the Capsule X material are shown in Table 5-5.

Irradiation of the vessel intermediate shell Plate B5012-1 material (transverse orientation) specimens to 1.38×10^{19} n/cm^2 (Figure 5-1) resulted in a 30 and 50 ft-lb transition temperature increase of 65 and 55°F respectively, and an upper shelf energy increase of 1 ft-lb when compared to the unirradiated data.[1]

Irradiation of the vessel intermediate shell Plate B5012-1 material (longitudinal orientation) specimens to 1.38×10^{19} n/cm^2 (Figure 5-2) resulted in a 30 and 50 ft-lb transition temperature increase of 45°F and an upper shelf energy decrease of 7 ft-lb when compared to the unirradiated data.[1]

Weld metal irradiated to 1.38×10^{19} n/cm^2 (Figure 5-3) resulted in a 30 and 50 ft-lb transition temperature increase of 165 and 185°F respectively and an upper shelf energy decrease of 29 ft-lb.

Weld HAZ metal irradiated to 1.38×10^{19} n/cm^2 (Figure 5-4) resulted in a 30 and 50 ft-lb transition temperature increase of 115 and 120°F respectively and an upper shelf energy decrease of 22 ft-lb.

The fracture appearance of each irradiated Charpy specimen from the various materials is shown in Figures 5-5 through 5-8 and show an increasing ductile or tougher appearance with increasing test temperature.

Table 5-6 shows a comparison of the 30 ft-lb transition temperature (ΔRT_{NDT}) increases for the various McGuire Unit 1 surveillance materials with predicted increases using the methods of NRC Regulatory Guide 1.99, Revision 2.[4] This comparison shows that the transition temperature increase resulting from irradiation to 1.38×10^{19} n/cm^2 is less than predicted by the Guide for Plate B5012-1 longitudinal specimens but 4°F higher than predicted for transverse specimens. The weld metal transition temperature increase resulting from 1.38×10^{19} n/cm^2 is less than the Guide prediction.

5-3. TENSION TEST RESULTS

The results of tension tests performed on Plate B5012-1 (transverse and longitudinal orientation) and weld metal irradiated to 1.38×10^{19} n/cm^2 are shown in Table 5-7 and Figures 5-9, 5-10 and 5-11, respectively. These results show that irradiation produced a 10 to 15 Ksi increase in 0.2 percent yield strength for Plate B5012-1 and 18 to 25 Ksi increase for the weld metal. Fractured tension specimens for each of the materials are shown in Figures 5-12, 5-13 and 5-14. A typical stress-strain curve for the tension specimens is shown in Figure 5-15.

5-4. COMPACT TENSION TESTS

Per the surveillance capsule testing contract with the Duke Power Company, 1/2T - Compact Tension Fracture Mechanics specimens will not be tested and will be stored at the Hot Cell at the Westinghouse R&D Center.

TABLE 5-1

CHARPY V-NOTCH IMPACT DATA FOR THE MCGUIRE UNIT 1
REACTOR VESSEL SHELL PLATE B5012-1
IRRADIATED AT 550°F, FLUENCE 1.38 x 10^{19} n/cm^2 (E > 1.0 MeV)

Sample No.	Temperature (°F)	(°C)	Impact Energy (ft-lb)	(J)	Lateral Expansion (mils)	(mm)	Shear (%)
			Longitudinal Orientation				
DL50	0	(-18)	8.0	(11.0)	7.0	(0.18)	5
DL55	25	(- 4)	18.0	(24.5)	13.0	(0.33)	10
DL51	40	(4)	25.0	(34.0)	21.0	(0.53)	10
DL47	50	(10)	35.0	(47.5)	26.0	(0.66)	15
DL53	50	(10)	39.0	(53.0)	29.0	(0.74)	20
DL60	74	(23)	44.0	(59.5)	33.0	(0.84)	30
DL59	74	(23)	55.0	(74.5)	36.0	(0.91)	30
DL57	100	(38)	62.0	(84.0)	84.0	(1.17)	40
DL54	125	(52)	73.0	(99.0)	56.0	(1.42)	60
DL46	150	(66)	85.0	(115.0)	68.0	(1.73)	75
DL58	200	(93)	105.0	(142.5)	72.0	(1.83)	85
DL49	250	(121)	136.0	(184.5)	80.0	(2.03)	100
DL52	300	(149)	121.0	(164.0)	79.0	(2.01)	100
DL48	350	(177)	134.0	(181.5)	90.0	(2.29)	100
DL56	400	(204)	140.0	(190.0)	79.0	(2.01)	100
			Transverse Orientation				
DT58	0	(-18)	13.0	(17.5)	12.0	(0.30)	10
DT54	25	(- 4)	19.0	(26.0)	18.0	(0.46)	15
DT57	50	(10)	19.0	(26.0)	19.0	(0.48)	20
DT52	60	(16)	15.0	(20.5)	18.0	(0.46)	20
DT53	74	(23)	49.0	(66.5)	37.0	(0.94)	35
DT50	74	(23)	35.0	(47.5)	26.0	(0.66)	25
DT60	100	(38)	56.0	(76.0)	46.0	(1.17)	45
DT49	100	(38)	45.0	(61.0)	38.0	(0.97)	40
DT55	125	(52)	49.0	(66.5)	42.0	(1.07)	50
DT59	150	(66)	62.0	(84.0)	50.0	(1.27)	60
DT47	200	(93)	94.0	(127.5)	69.0	(1.75)	100
DT56	250	(121)	103.0	(139.5)	74.0	(1.88)	100
DT48	300	(149)	113.0	(153.0)	81.0	(2.06)	100
DT51	350	(177)	93.0	(126.0)	76.0	(1.93)	100
DT46	400	(204)	109.0	(148.0)	76.0	(1.93)	100

TABLE 5-2

CHARPY V-NOTCH IMPACT DATA FOR THE MCGUIRE UNIT 1
REACTOR VESSEL WELD METAL AND HAZ METAL IRRADIATED AT 550°F
FLUENCE 1.38 x 10^{19} n/cm^2 (E > 1.0 MeV)

Sample No.	Temperature (°F)	(°C)	Impact Energy (ft-lb)	(J)	Lateral Expansion (mils)	(mm)	Shear (%)
			Weld Metal				
DW21	74	(23)	14.0	(19.0)	19.0	(0.48)	15
DW49	100	(38)	15.0	(20.5)	14.0	(0.36)	20
DW53	125	(52)	17.0	(23.0)	20.0	(0.51)	20
DW56	150	(66)	29.0	(39.5)	28.0	(0.71)	35
DW59	150	(66)	MACHINE MALFUNCTION			-	-
DW50	150	(66)	33.0	(44.5)	28.0	(0.71)	40
DW58	175	(79)	38.0	(51.5)	27.0	(0.69)	50
DW46	175	(79)	39.0	(53.0)	34.0	(0.86)	65
DW60	200	(93)	39.0	(53.0)	36.0	(0.91)	65
DW57	210	(99)	43.0	(58.5)	34.0	(0.86)	75
DW52	225	(107)	83.0	(112.5)	57.0	(1.45)	100
DW48	225	(107)	MACHINE MALFUNCTION			-	-
DW47	300	(149)	87.0	(118.0)	63.0	(1.60)	100
DW55	350	(177)	83.0	(112.5)	67.0	(1.70)	100
DW54	400	(204)	79.0	(107.0)	64.0	(1.63)	100
			HAZ Metal				
DH46	- 25	(-32)	9.0	(12.0)	9.0	(0.23)	10
DH54	25	(- 4)	15.0	(20.5)	11.0	(0.28)	15
DH52	40	(4)	26.0	(35.5)	17.0	(0.43)	20
DH58	50	(10)	28.0	(38.0)	24.0	(0.61)	30
DH53	50	(10)	34.0	(46.0)	24.0	(0.61)	30
DH55	74	(23)	33.0	(44.5)	29.0	(0.74)	40
DH50	74	(23)	54.0	(73.0)	34.0	(0.86)	50
DH48	100	(38)	32.0	(43.5)	23.0	(0.61)	35
DH56	125	(52)	53.0	(72.0)	45.0	(1.14)	50
DH47	150	(66)	77.0	(104.5)	58.0	(1.47)	75
DH49	200	(93)	59.0	(80.0)	52.0	(1.32)	60
DH51	250	(121)	92.0	(124.5)	71.0	(1.80)	100
DH59	300	(149)	109.0	(148.0)	74.0	(1.88)	100
DH57	350	(177)	95.0	(129.0)	75.0	(1.88)	100
DH60	400	(204)	88.0	(119.5)	66.0	(1.68)	100

TABLE 5-3

INSTRUMENTED CHARPY IMPACT TEST RESULTS FOR MCGUIRE UNIT 1

REACTOR VESSEL SHELL PLATE B5012-1

Sample Number	Test Temp (°F)	Charpy Energy (ft-lb)	Normalized Energies (ft-lb/in^2): Charpy Ed/A	Maximum Em/A	Prop Ep/A	Yield Load (kips)	Time to Yield (μsec)	Maximum Load (kips)	Time to Maximum (μsec)	Fracture Load (kips)	Arrest Load (kips)	Yield Stress (ksi)	Flow Stress (ksi)
						Longitudinal Orientation							
DL50	0	8.0	64	33	31	3.50	25	3.90	250	3.90	-	-1	64
DL55	25	18.0	145	60	85	1.50	50	3.90	405	3.85	0.38	50	89
DL51	40	25.0	201	149	53	3.25	0	4.15	580	4.15	-	0	69
DL47	50	35.0	282	171	111	3.10	20	3.95	774	3.85	-	[illegible]	65
DL53	50	39.0	314	252	62	3.05	85	4.95	530	4.55	0.15	101	126
DL60	74	44.0	354	224	131	3.10	120	4.35	530	4.35	0.60	102	123
DL59	74	55.0	443	311	132	2.20	50	4.50	655	4.40	0.85	73	111
DL57	100	62.0	499	269	230	3.00	15	4.10	1065	4.05	0.90	0	68
DL54	125	73.0	588	364	224	3.60	40	4.40	945	4.10	2.00	36	91
DL46	150	85.0	684	271	414	3.35	110	4.30	605	3.75	2.20	108	125
DL58	200	105.0	845	282	563	2.85	25	4.10	740	3.10	2.15	-1	67
DL49	250	136.0	1095	319	776	2.55	40	4.10	785	-	-	50	93
DL52	300	121.0	974	299	675	2.85	100	3.95	720	-	-	93	112
DL48	350	134.0	1079	253	826	2.40	150	3.60	720	-	-	79	99
DL56	400	140.0	1127	297	830	2/65	95	3.80	740	-	-	88	107
						Transverse Orientation							
DT58	0	13.0	105	70	34	3.55	10	4.00	320	3.95	-	0	66
DT54	25	19.0	153	108	45	3.20	25	3.65	570	3.65	-	-1	60
DT57	50	19.0	153	95	58	3.00	15	3.50	805	3.50	0.35	0	58
DT52	60	15.0	121	40	81	3.00	10	3.45	450	3.15	0.55	-1	57
DT50	74	35.0	282	180	101	3.20	55	4.30	580	4.25	0.25	0	71
DT53	74	49.0	395	216	179	3.15	55	4.35	470	4.35	1.15	104	124
DT49	100	45.0	362	209	154	3.00	20	4.30	550	4.10	1.15	41	90
DT60	100	56.0	451	293	158	3.15	40	4.25	905	4.20	1.15	0	70
DT55	125	49.0	395	247	148	2.76	30	4.10	740	4.05	1.35	-1	67
DT59	150	62.0	500	COMPUTER MALFUNCTION			-	-	-	-	-	-	-
DT47	200	94.0	757	277	480	0.00	25	4.10	980	-	-	0	67
DT56	250	103.0	829	259	571	2.65	60	3.95	630	-	-	87	109
DT48	300	113.0	910	254	656	2.50	65	3.90	625	-	-	82	106
DT51	350	93.0	749	224	525	0.00	10	3.80	870	-	-	0	63
DT46	400	109.0	878	244	634	2.20	25	3.85	605	-	-	73	100

3887s/081489:10

TABLE 5-4

INSTRUMENTED CHARPY IMPACT TEST RESULTS FOR MCGUIRE UNIT 1

REACTOR VESSEL WELD METAL AND HAZ METAL

Sample Number	Test Temp (°F)	Charpy Energy (ft-lb)	Normalized Energies (ft-lb/in^2): Charpy Ed/A	Normalized Energies (ft-lb/in^2): Maximum Em/A	Normalized Energies (ft-lb/in^2): Prop Ep/A	Yield Load (kips)	Time to Yield (μsec)	Maximum Load (kips)	Time to Maximum (μsec)	Fracture Load (kips)	Arrest Load (kips)	Yield Stress (ksi)	Flow Stress (ksi)
							Weld Metal						
DW51	74	14.0	113	44	69	2.60	55	3.80	130	3.80	0.25	86	106
DW49	100	15.0	121	61	60	3.40	20	3.60	795	3.60	0.35	0	59
DW53	125	17.0	137	68	69	3.00	10	3.40	700	3.35	0.70	-1	56
DW56	150	29.0	234	142	92	3.30	5	3.80	560	3.80	1.40	0	62
DW59	150	MACHINE MALFUNCTION		-	-	-	-	-	-	-	-	-	-
DW50	150	33.0	266	180	86	3.50	10	4.10	665	4.10	1.30	-1	68
DW58	175	38.0	306	211	95	3.00	15	4.05	755	4.05	1.70	0	67
DW46	175	39.0	314	172	142	3.40	20	4.05	655	4.05	2.40	0	67
DW60	200	39.0	314	177	137	3.25	15	4.00	915	3.85	1.70	0	66
DW57	210	43.0	346	217	129	3.10	0	4.10	700	4.10	2.30	0	67
DW52	225	83.0	668	229	440	3.2	170	4.25	570	-	-	105	123
DW48	225	MACHINE MALFUNCTION		-	-	-	-	-	-	-	-	-	-
DW47	300	87.0	701	244	457	0.00	5	4.05	870	-	-	0	67
DW55	350	83.0	668	237	432	-7.45	20	3.95	840	-	-	-1	65
DW54	400	79.0	636	221	415	-7.45	5	3.95	855	-	-	-1	65
							HAZ Metal						
DH46	- 25	9.0	72	51	21	3.40	65	3.75	145	4.05	0.20	88	106
DH54	25	15.0	121	40	80	3.70	5	3.50	435	3.50	0.85	0	58
DH52	40	26.0	209	119	91	3.60	5	4.20	460	4.20	0.95	0	69
DH58	50	28.0	225	118	107	3.60	50	4.20	335	4.20	1.75	50	94
DH53	50	34.0	274	144	130	3.30	10	3.95	675	3.90	1.30	-1	65
DH55	74	33.0	266	117	149	3.60	5	4.15	545	4.15	2.85	0	68
DH50	74	54.0	435	225	209	3.40	45	4.50	460	4.40	2.50	112	130
DH48	100	32.0	258	192	66	3.40	85	4.25	425	4.25	1.05	112	127
DH56	125	53.0	427	236	191	3.50	10	4.45	740	4.35	3.05	-1	73
DH47	150	77.0	620	287	333	3.00	5	4.20	750	4.10	3.75	0	69
DH49	200	59.0	475	293	182	3.25	10	4.10	1215	3.95	1.95	0	68
DH51	250	92.0	741	287	454	3.15	120	4.10	705	0.25	0.25	76	106
DH59	300	109.0	878	313	565	3.00	5	4.00	1175	-	-	0	66
DH57	350	95.0	765	265	500	2.50	50	4.05	620	-	-	83	109
DH60	400	88.0	709	199	510	3.10	15	3.08	800	-	-	-1	62

TABLE 5-5
THE EFFECT OF 550°F IRRADIATION AT 1.38 x 10^{19} n/cm^2 (E > 1.0 MeV)
ON THE NOTCH TOUGHNESS PROPERTIES OF THE
MCGUIRE UNIT 1 REACTOR VESSEL MATERIALS

	Average 30 ft-lb Temp (°F)			Average 35 mil Lateral Expansion Temp (°F)			Average 50 ft-lb Temp (°F)			Average Energy Absorption at Full Shear (ft-lb)		
Material	Unirradiated	Irradiated	ΔT	Unirradiated	Irradiated	ΔT	Unirradiated	Irradiated	ΔT	Unirradiated	Irradiated	Δ(ft-lb)
Plate B5012-1 (Longitudinal)	5	50	45	35	75	40	35	80	45	140	133	-7
Plate B5012-1 (Transverse)	0	65	65	50	95	45	75	130	55	101	102	+1
Weld Metal	-5	160	165	0	190	190	20	205	185	112	83	-29
HAZ Metal	-50	65	115	-15	100	115	-5	115	120	118	96	-22

TABLE 5-6

COMPARISON OF MCGUIRE UNIT 1
REACTOR VESSEL SURVEILLANCE CAPSULE CHARPY IMPACT TEST RESULTS
WITH REGULATORY GUIDE 1.99 REVISION 2 PREDICTIONS

			ΔRT_{NDT} (°F)		USE DECREASE (%)	
Material	Capsule	Fluence 10^{19} n/cm^2	Meas.	R.G 1.99 Pred.	Meas.	R.G 1.99 Pred.
Plate B5012-1	U	0.414	45	42	5	15
(Longitudinal)	X	1.38	45	61	5	20
Plate B5012-1	U	0.414	50	42	1	15
(Transverse)	X	1.38	65	61	0	20
Weld Metal	U	0.414	160	159	33	28
	X	1.38	165	229	26	37

TABLE 5-7

TENSILE PROPERTIES FOR MCGUIRE UNIT 1

REACTOR VESSEL MATERIAL IRRADIATED TO 1.38 x 10^{19} n/cm^2 (E > 1.0 MeV)

Material	Sample Number	Test Temp. (°F)	0.2% Yield Strength (ksi)	Ultimate Strength (ksi)	Fracture Load (kip)	Fracture Stress (ksi)	Fracture Strength (ksi)	Uniform Elongation (%)	Total Elongation (%)	Reduction in Area (%)
Plate B5012-1 (Long. Orient.)	DL11	74	78.9	98.9	3.10	175.4	63.2	10.5	25.2	64
	DL12	200	75.4	94.7	3.05	178.5	62.1	9.8	22.2	65
	DL10	550	69.8	91.7	3.10	208.8	63.2	9.8	21.2	57
Plate B5012-1 (Transv. Orient.)	DT11	74	76.4	95.8	3.45	171.6	70.3	12.0	24.6	64
	DT12	200	73.3	91.5	3.10	180.2	63.2	10.5	23.1	64
	DT10	550	67.0	90.7	3.65	132.2	74.4	9.0	12.9	60
Weld	DW11	175	84.0	97.8	3.45	216.3	70.3	12.0	24.1	68
	DW12	225	78.4	89.6	3.35	189.6	68.2	10.5	20.9	64
	DW10	550	77.4	94.3	3.30	174.9	67.2	9.0	19.1	62

Curve 757276-A

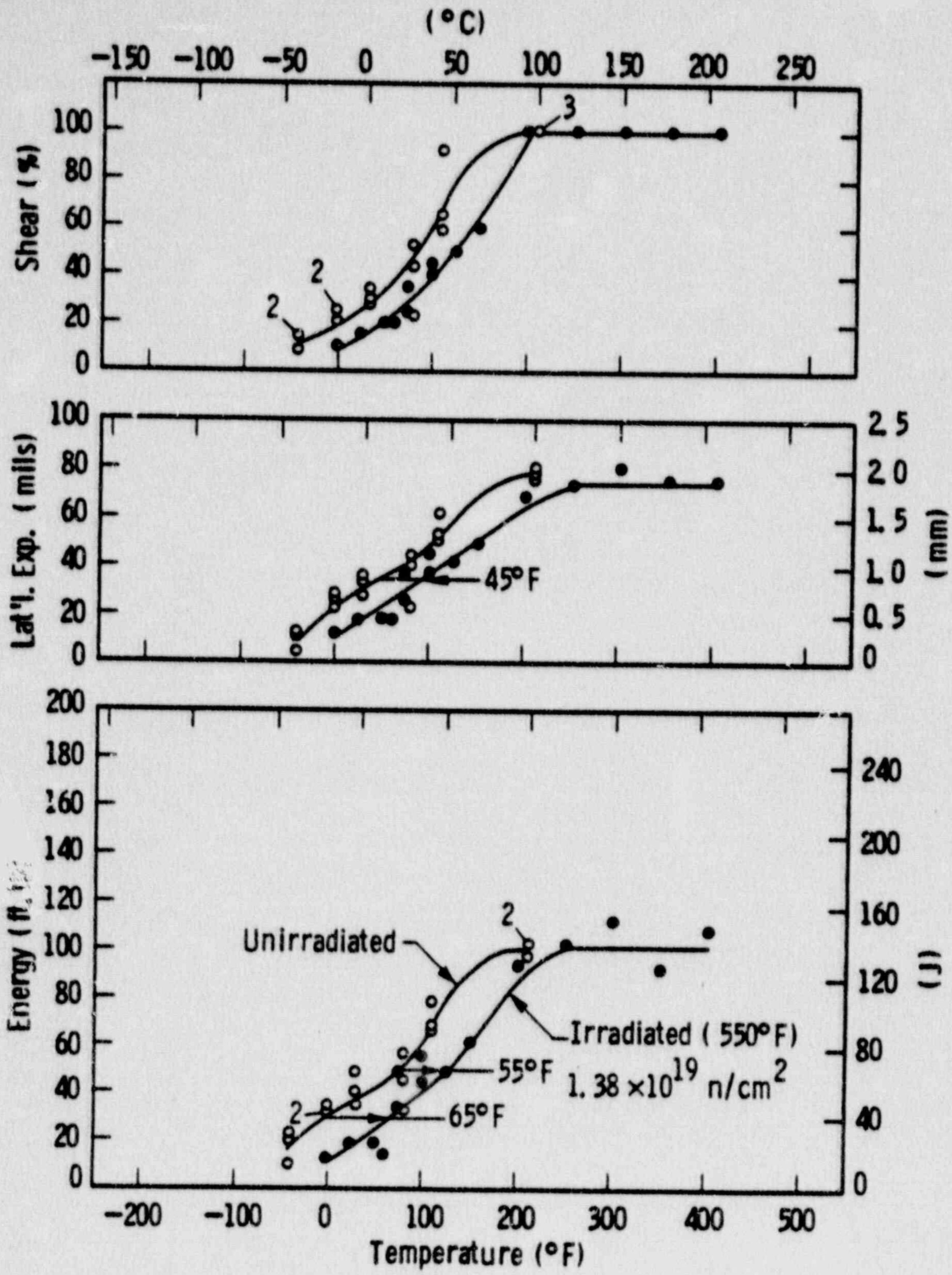

FIGURE 5-1 CHARPY V-NOTCH IMPACT DATA FOR MCGUIRE UNIT 1 REACTOR VESSEL SHELL PLATE B5012-1 (TRANSVERSE ORIENTATION)

Curve 757277-A

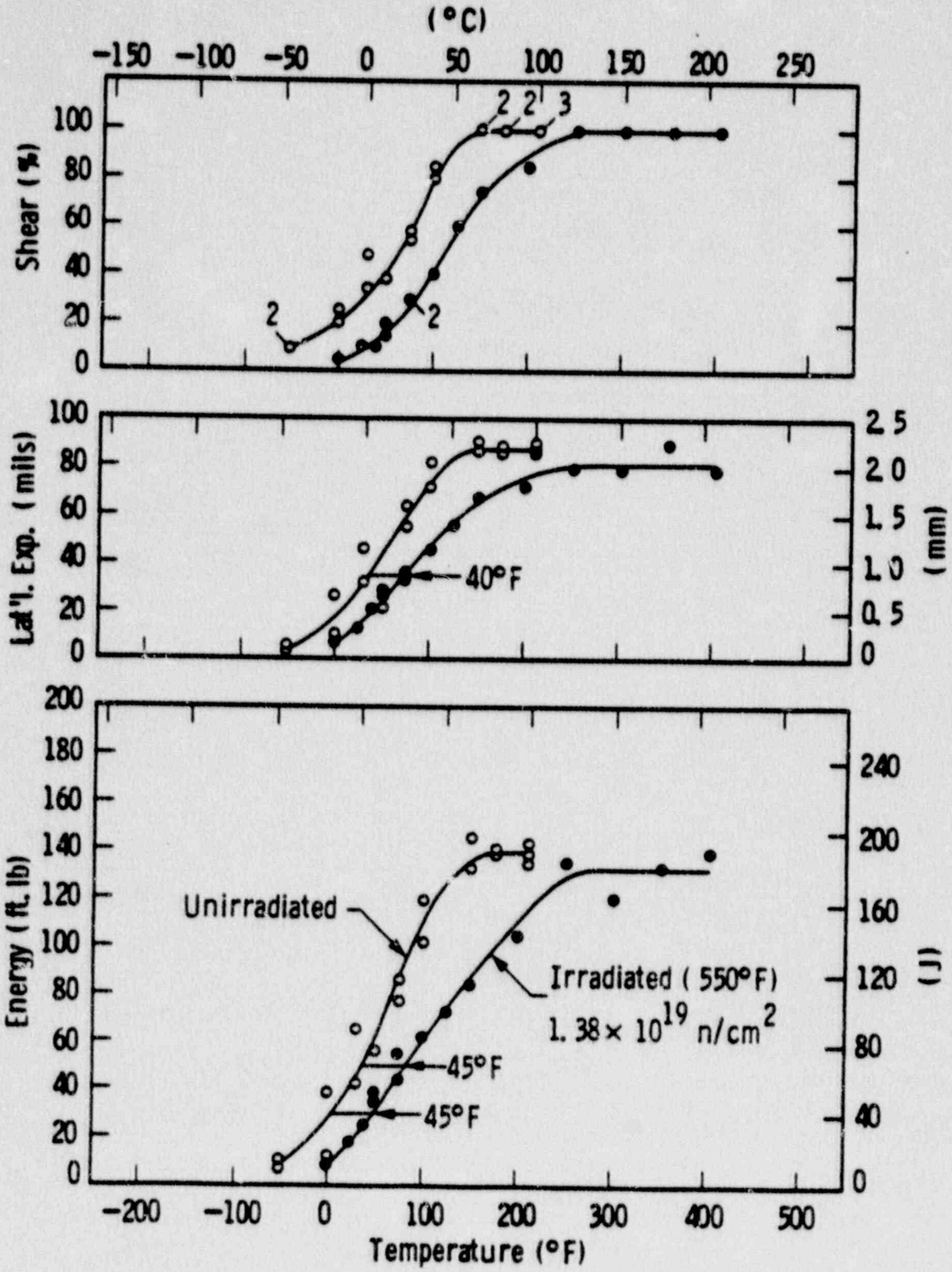

FIGURE 5-2 CHARPY V-NOTCH IMPACT DATA FOR MCGUIRE UNIT 1 REACTOR VESSEL SHELL PLATE B5012-1 (LONGITUDINAL ORIENTATION)

Curve 757278-A

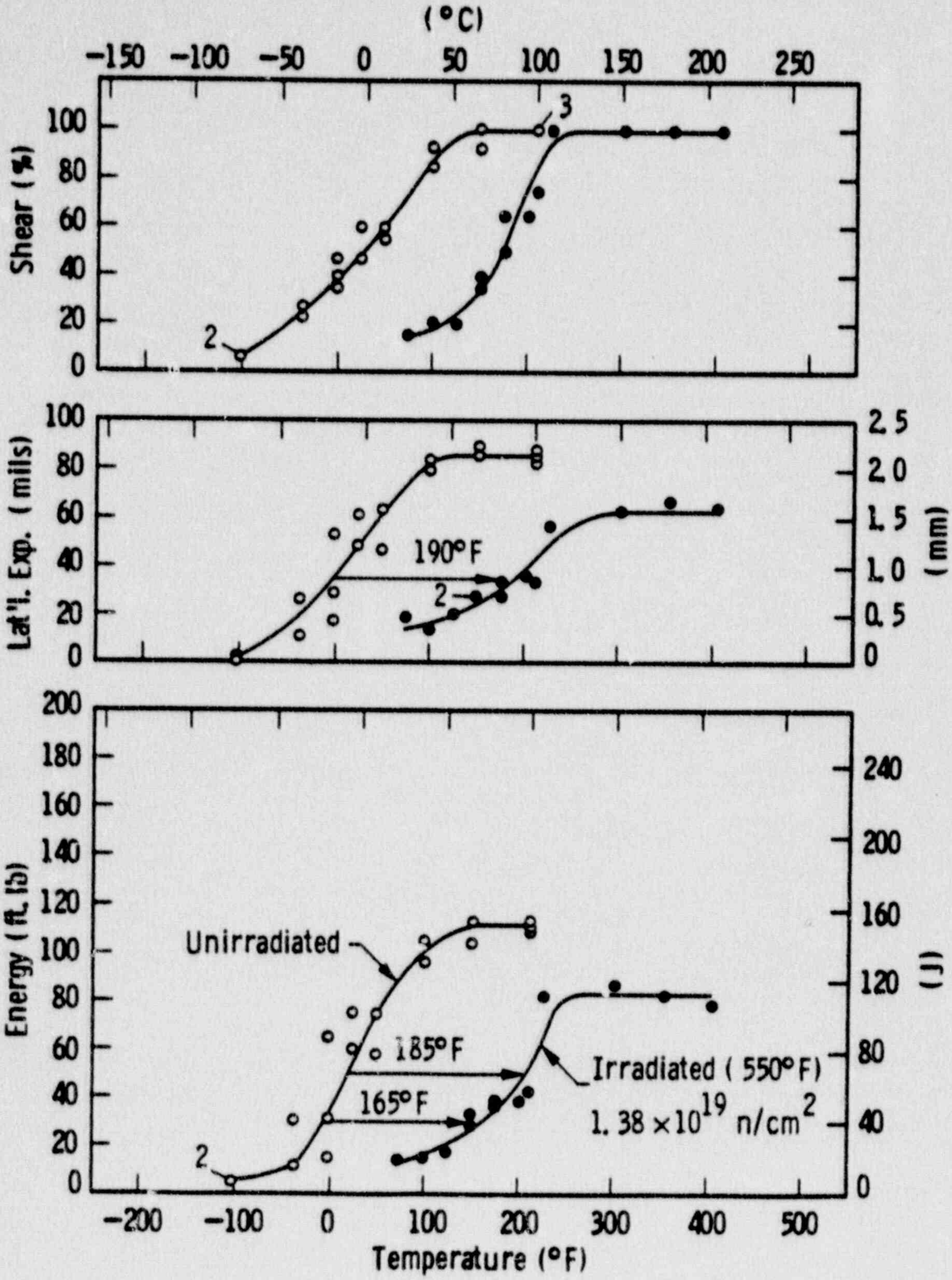

FIGURE 5-3 CHARPY V-NOTCH IMPACT DATA FOR MCGUIRE UNIT 1 REACTOR VESSEL WELD METAL

Curve 757279-A

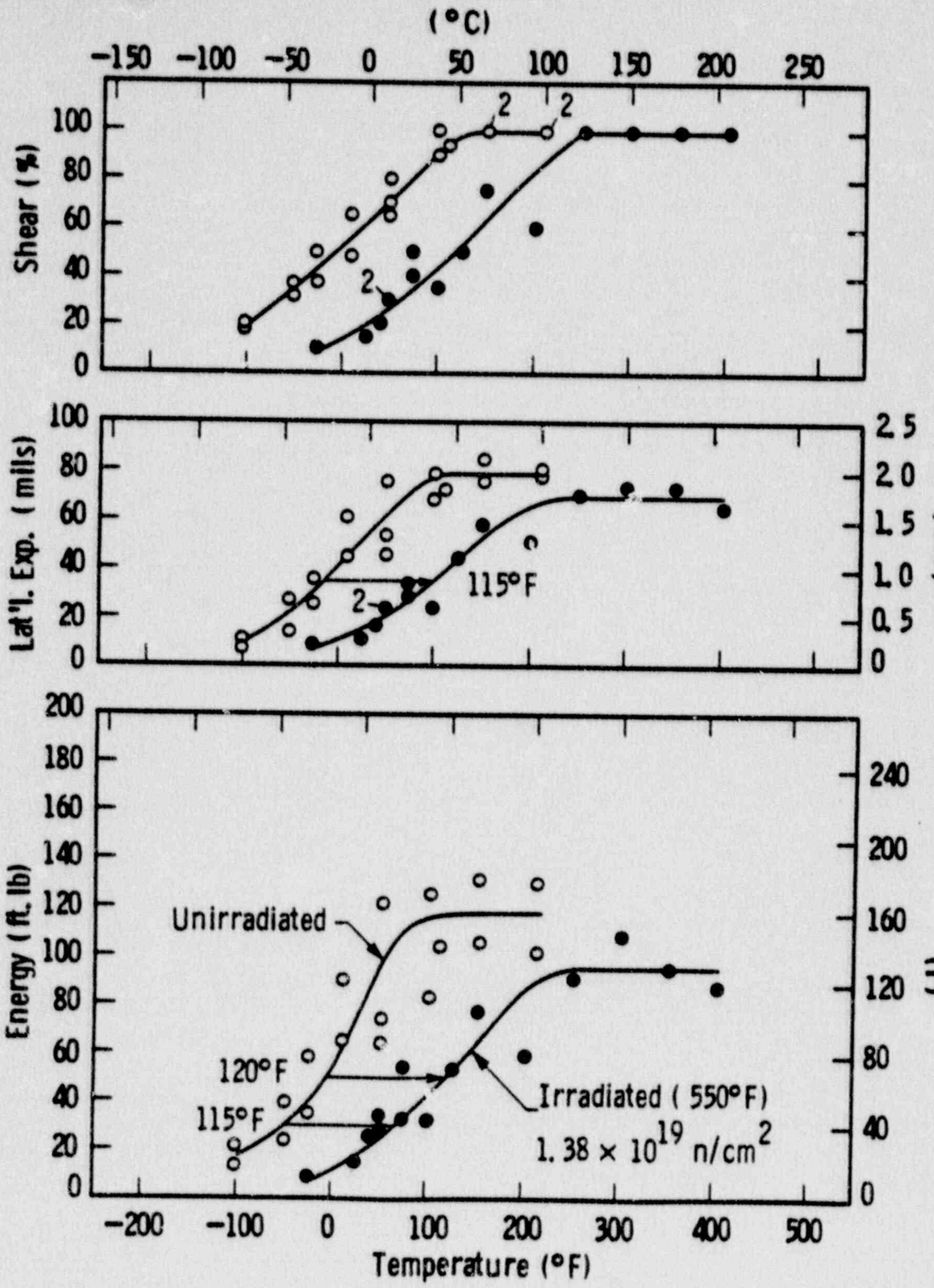

FIGURE 5-4 CHARPY V-NOTCH IMPACT DATA FOR MCGUIRE UNIT 1 REACTOR VESSEL WELD HEAT AFFECTED ZONE METAL

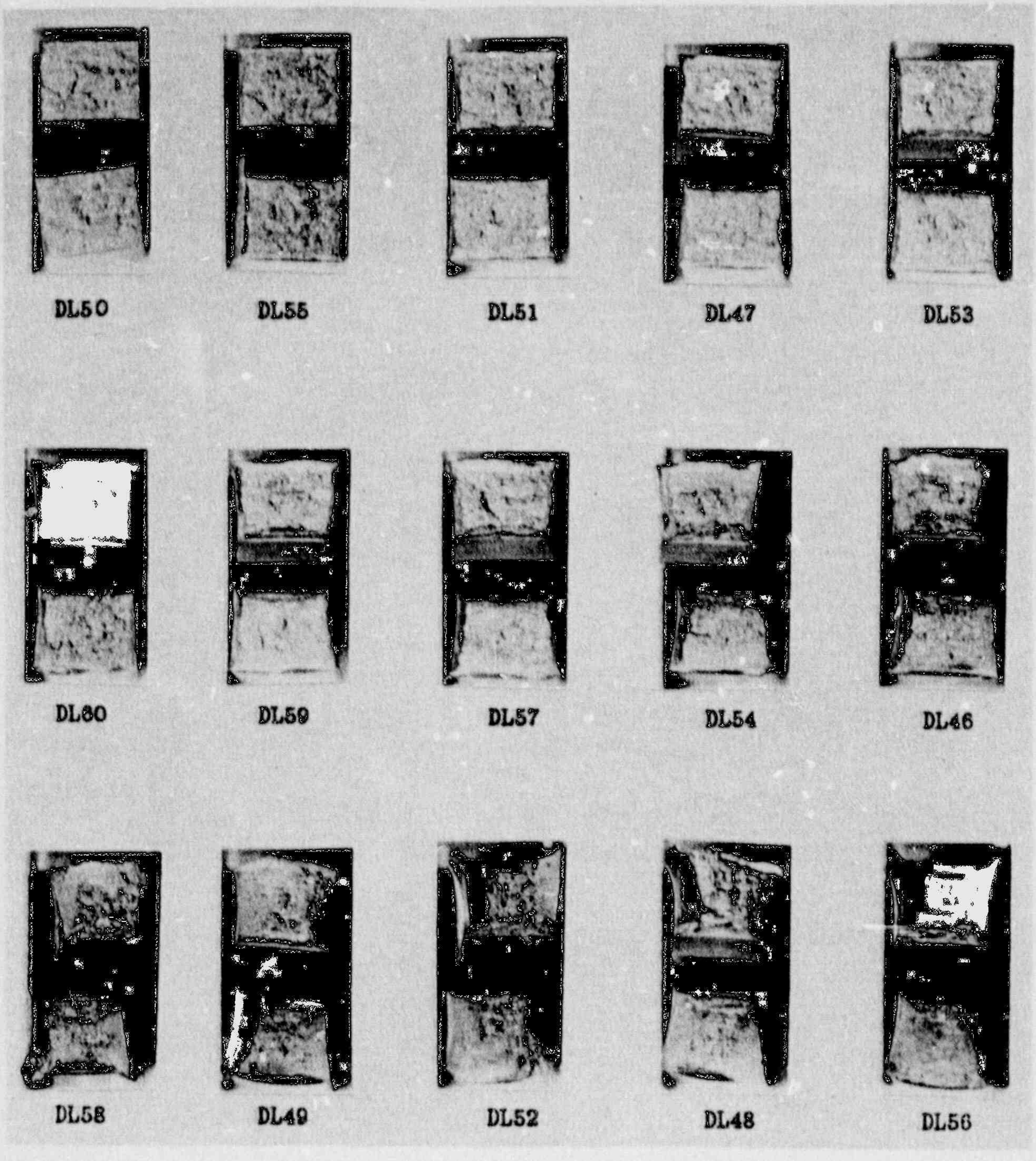

FIGURE 5-5 CHARPY IMPACT SPECIMEN FRACTURE SURFACES FOR MCGUIRE UNIT 1 REACTOR VESSEL SHELL PLATE B5012-1 (LONGITUDINAL ORIENTATION)

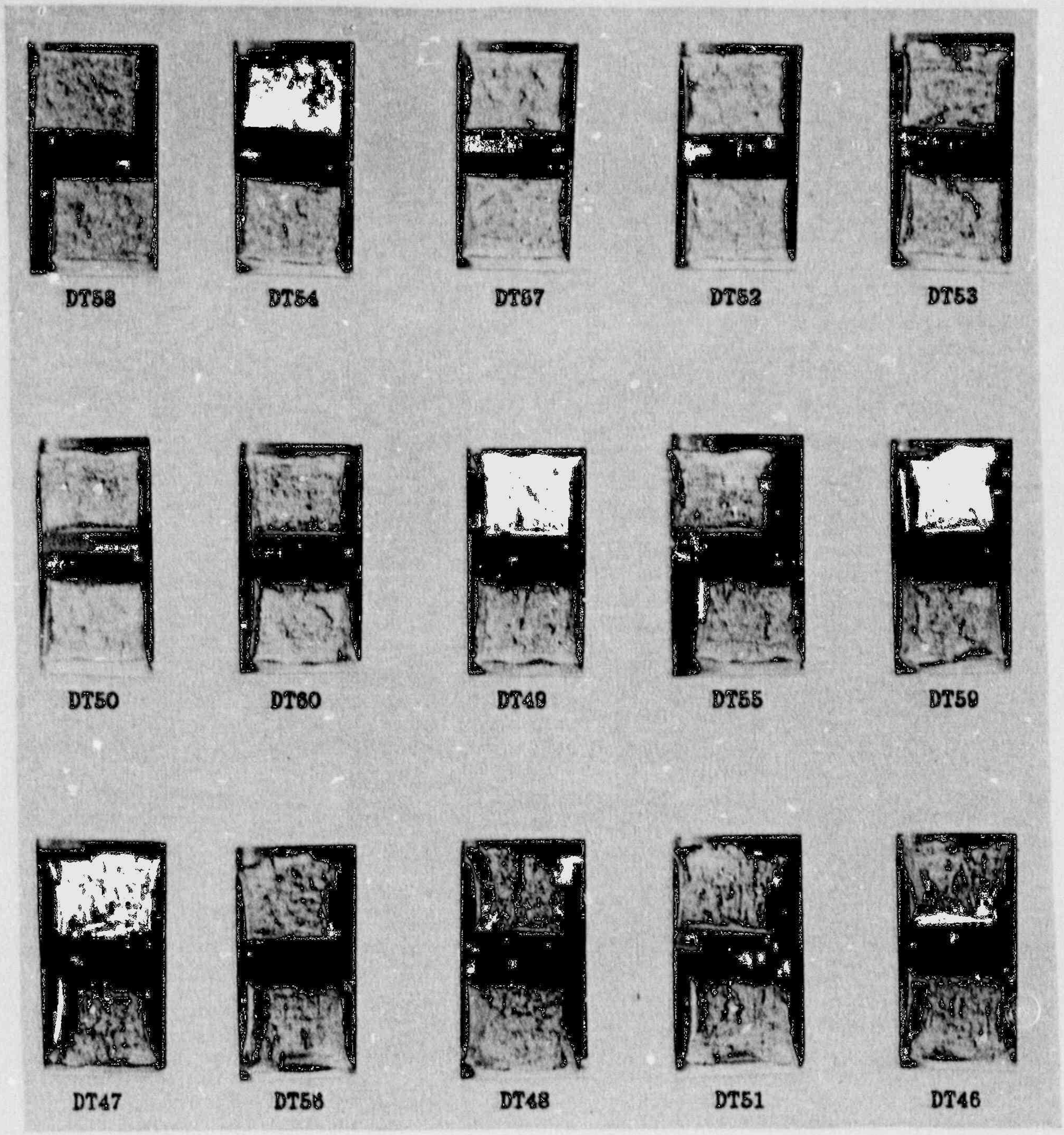

FIGURE 5-6 CHARPY IMPACT SPECIMEN FRACTURE SURFACES FOR MCGUIRE UNIT 1 REACTOR VESSEL SHELL PLATE B5012-1 (TRANSVERSE ORIENTATION)

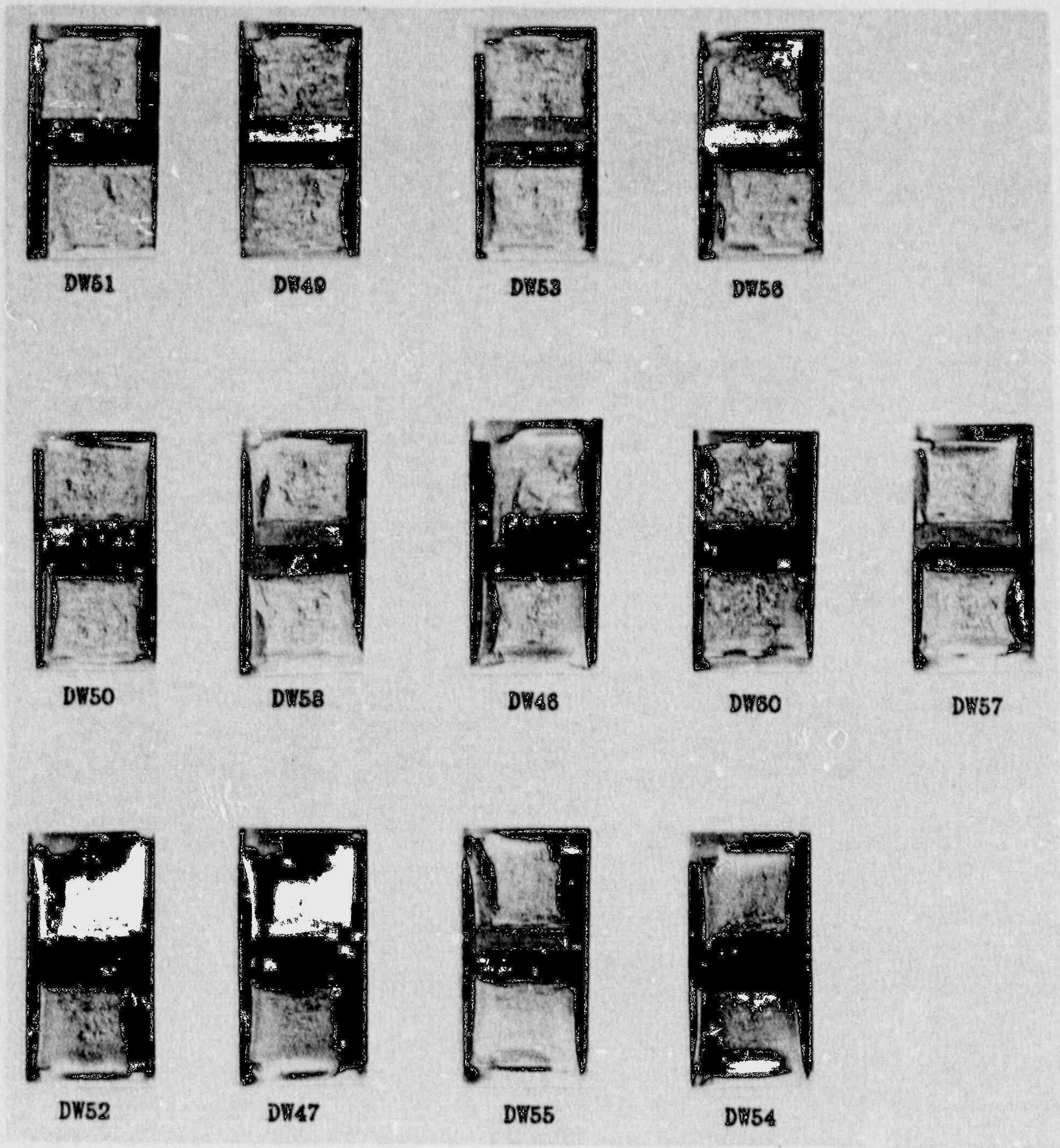

FIGURE 5-7 CHARPY IMPACT SPECIMEN FRACTURE SURFACES FOR MCGUIRE UNIT 1 REACTOR VESSEL WELD METAL

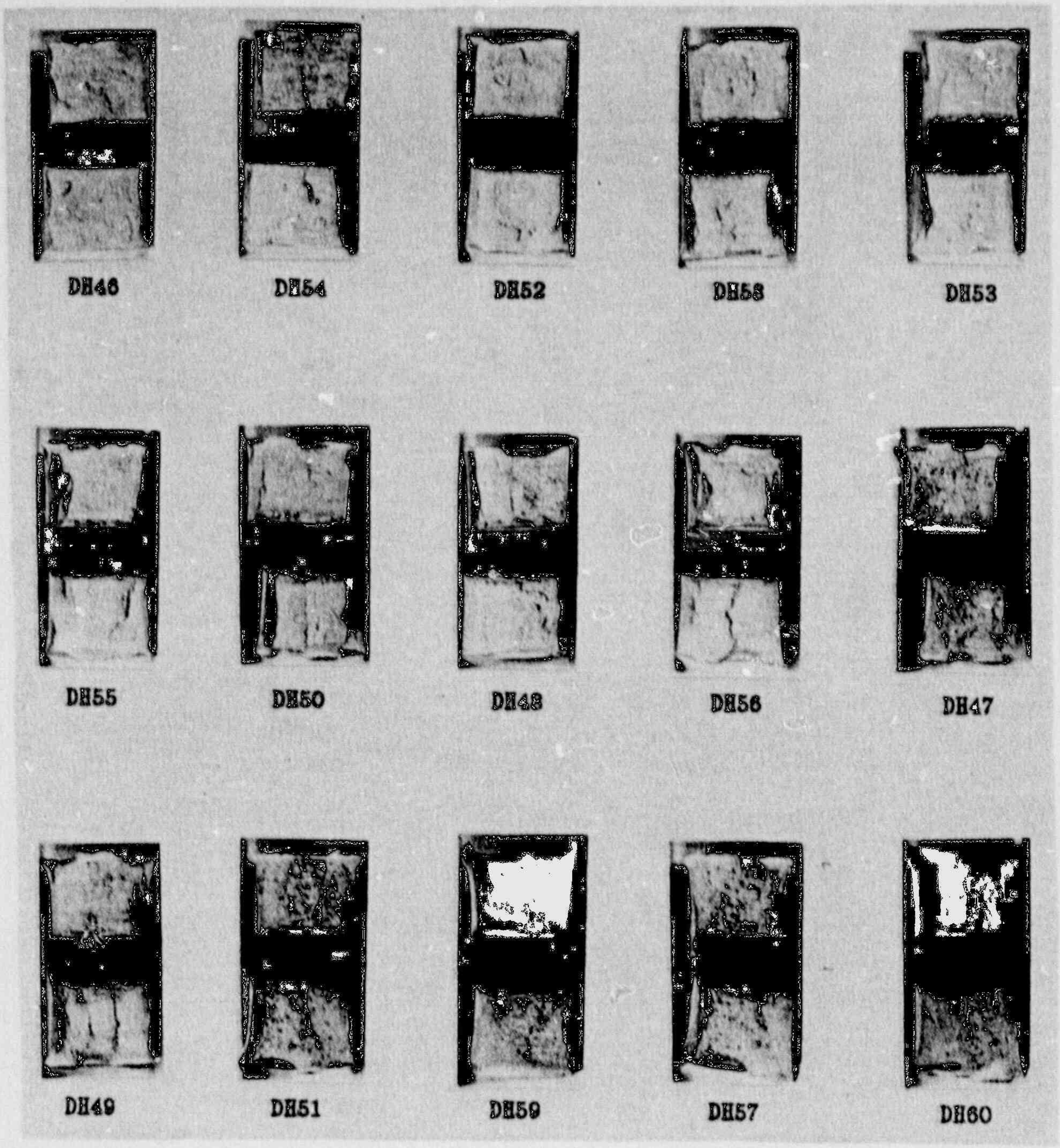

FIGURE 5-8 CHARPY IMPACT SPECIMEN FRACTURE SURFACES FOR MCGUIRE UNIT 1 REACTOR VESSEL WELD HAZ METAL

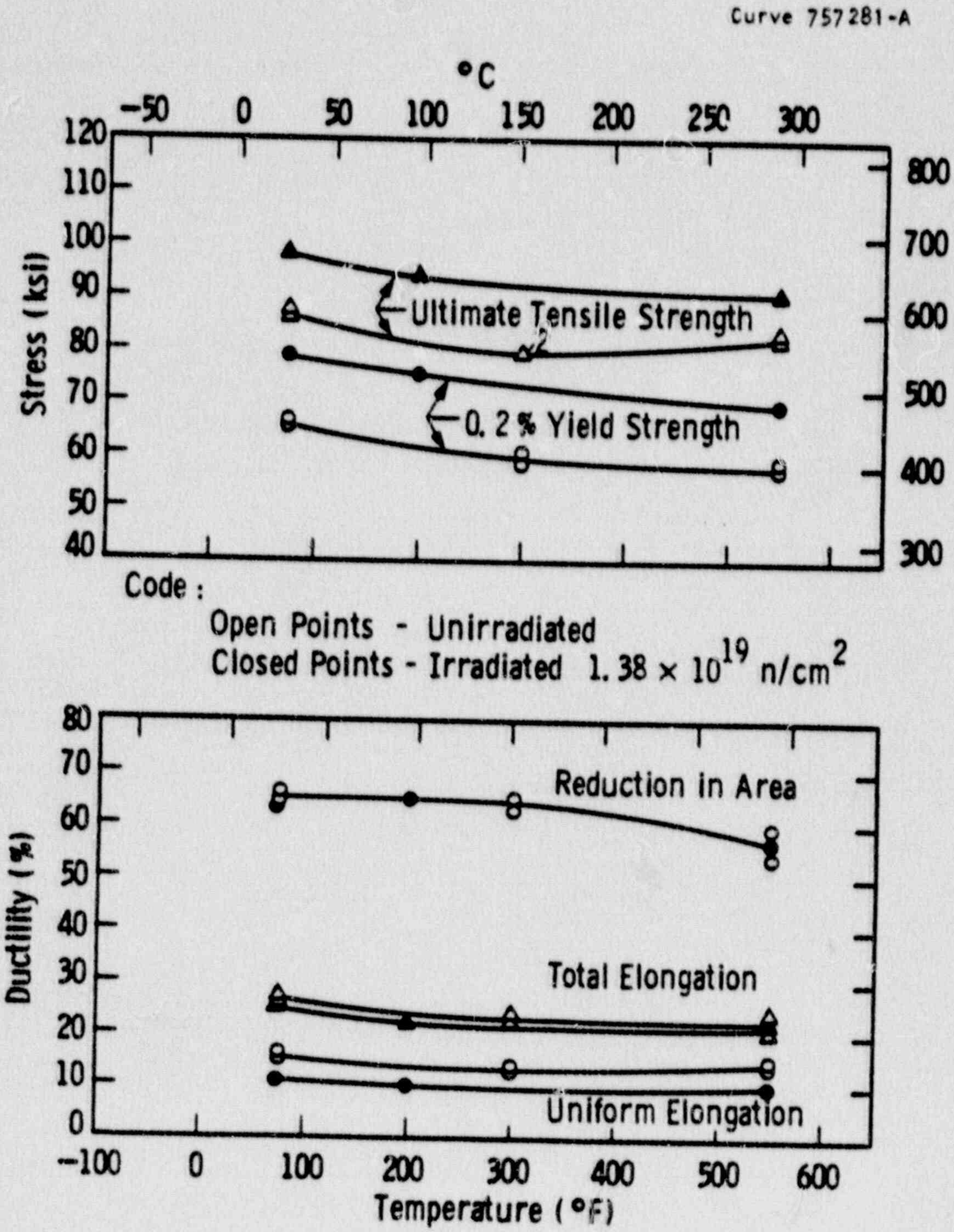

FIGURE 5-9 TENSILE PROPERTIES FOR MCGUIRE UNIT 1 REACTOR VESSEL SHELL PLATE B5012-1 (LONGITUDINAL ORIENTATION)

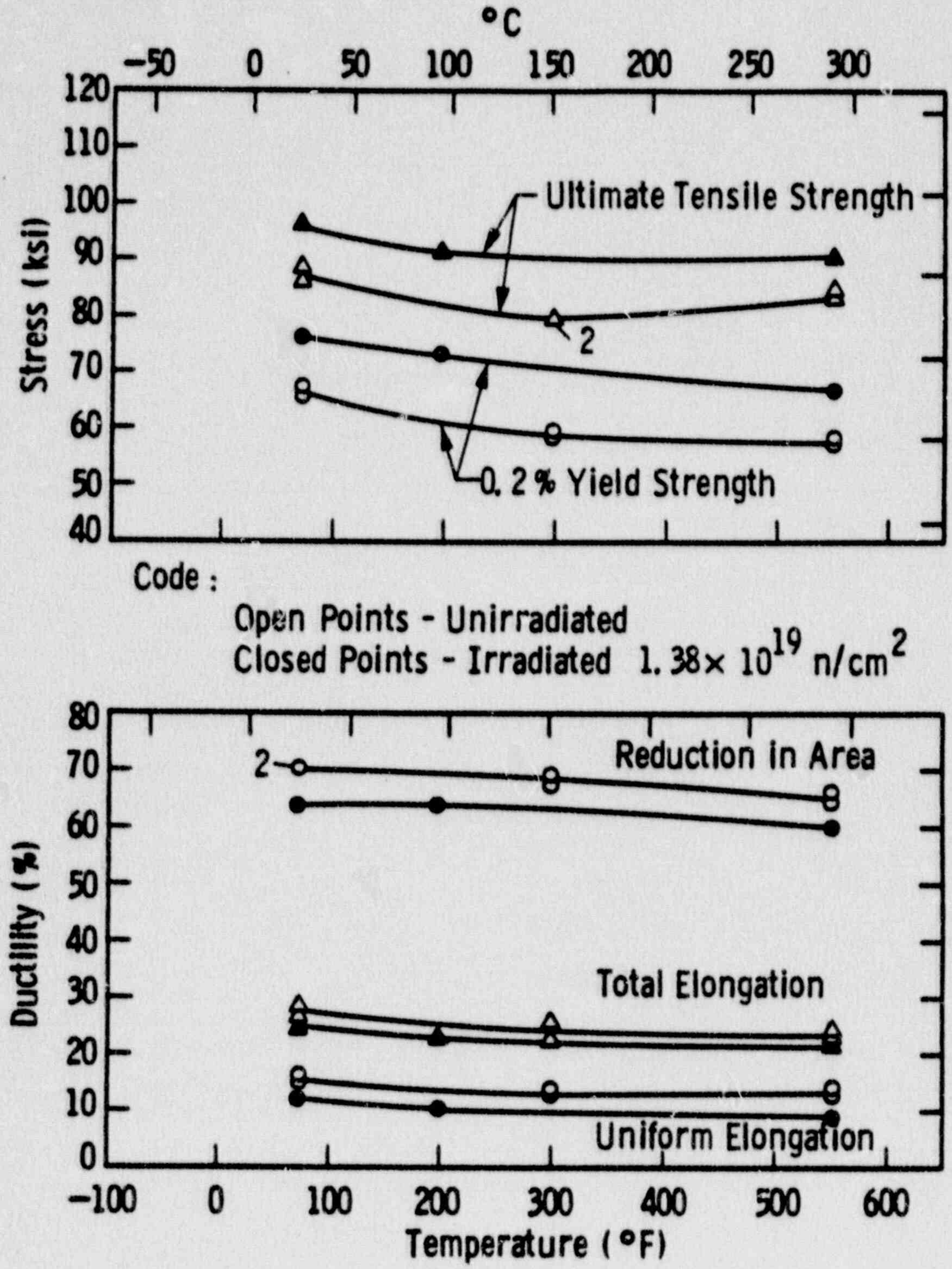

FIGURE 5-10 TENSILE PROPERTIES FOR MCGUIRE UNIT 1 REACTOR VESSEL SHELL PLATE B5012-1 (TRANSVERSE ORIENTATION)

Curve 757280-A

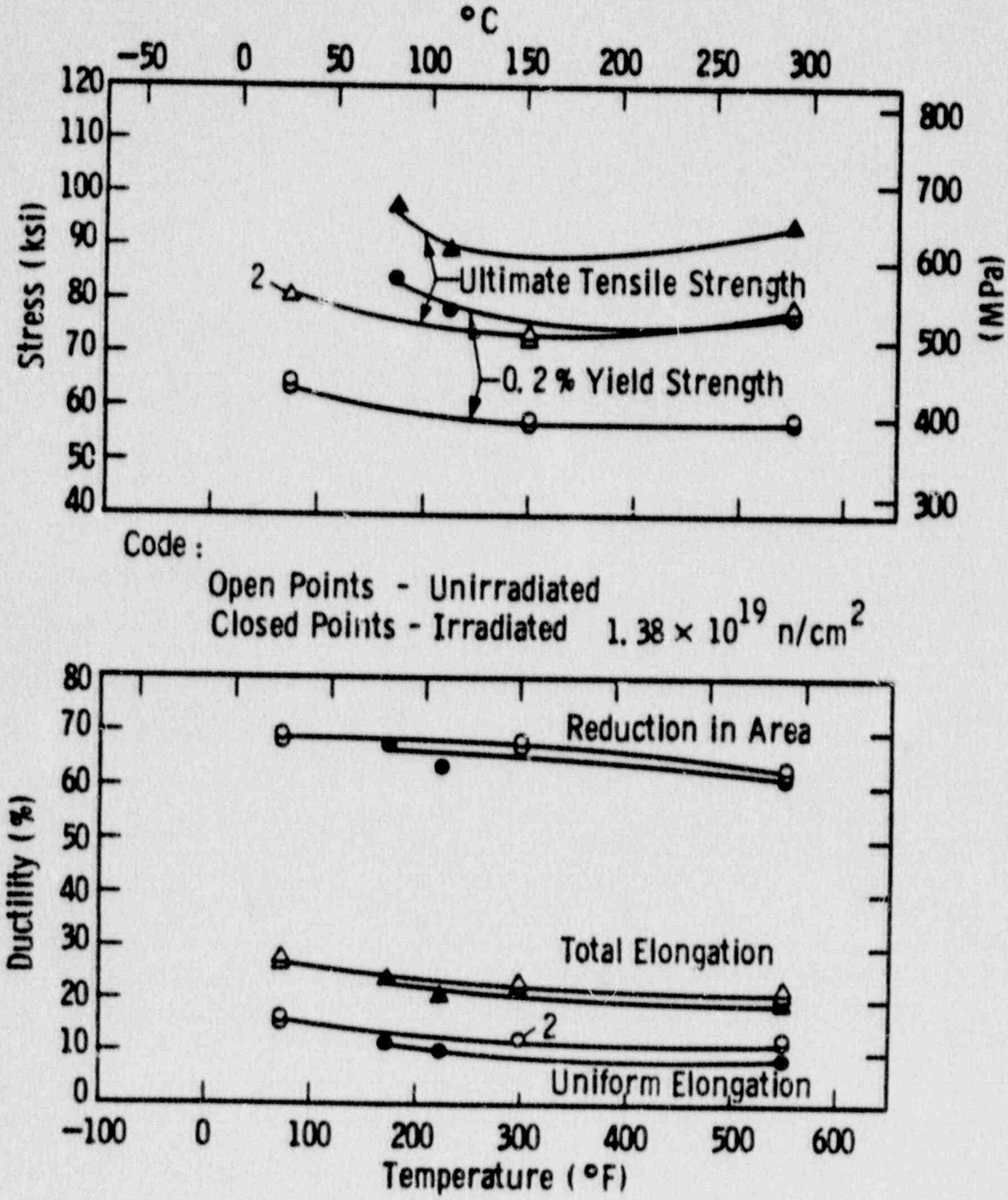

FIGURE 5-11 TENSILE PROPERTIES FOR MCGUIRE UNIT 1 REACTOR VESSEL WELD METAL

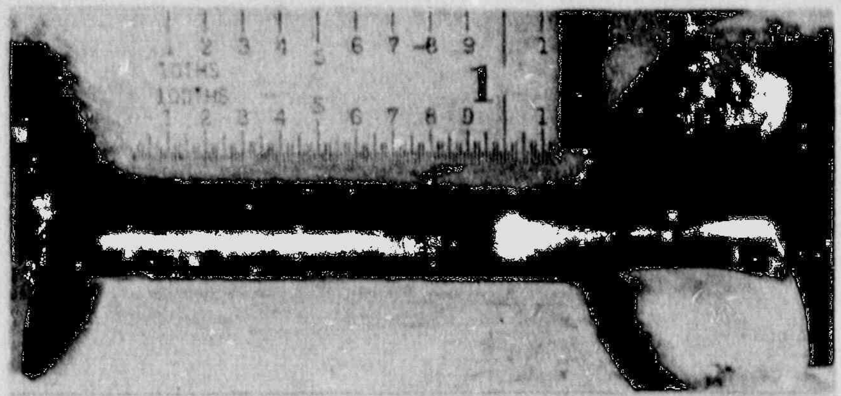

Specimen DL11 74°F

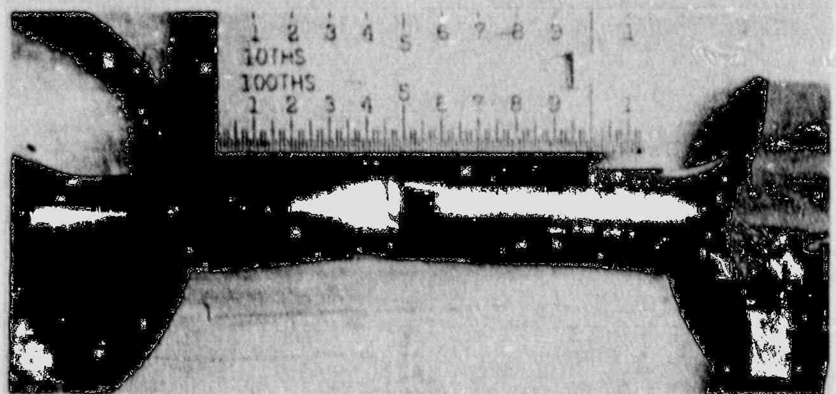

Specimen DL12 200°F

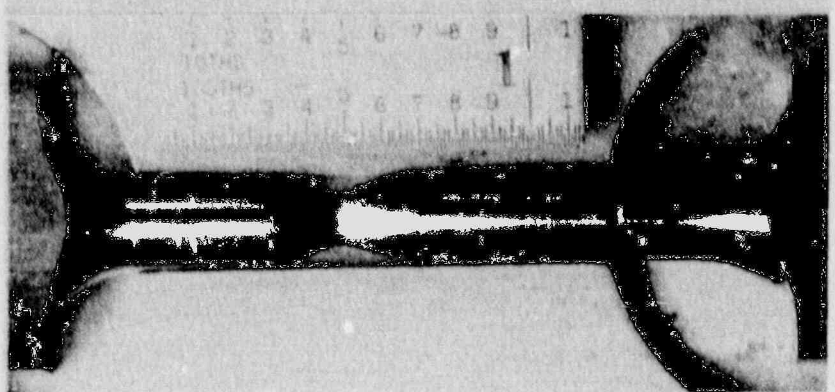

Specimen DL10 550°F

FIGURE 5-12 FRACTURED TENSILE SPECIMENS FOR MCGUIRE UNIT 1 REACTOR VESSEL SHELL PLATE B5012-1 (LONGITUDINAL ORIENTATION)

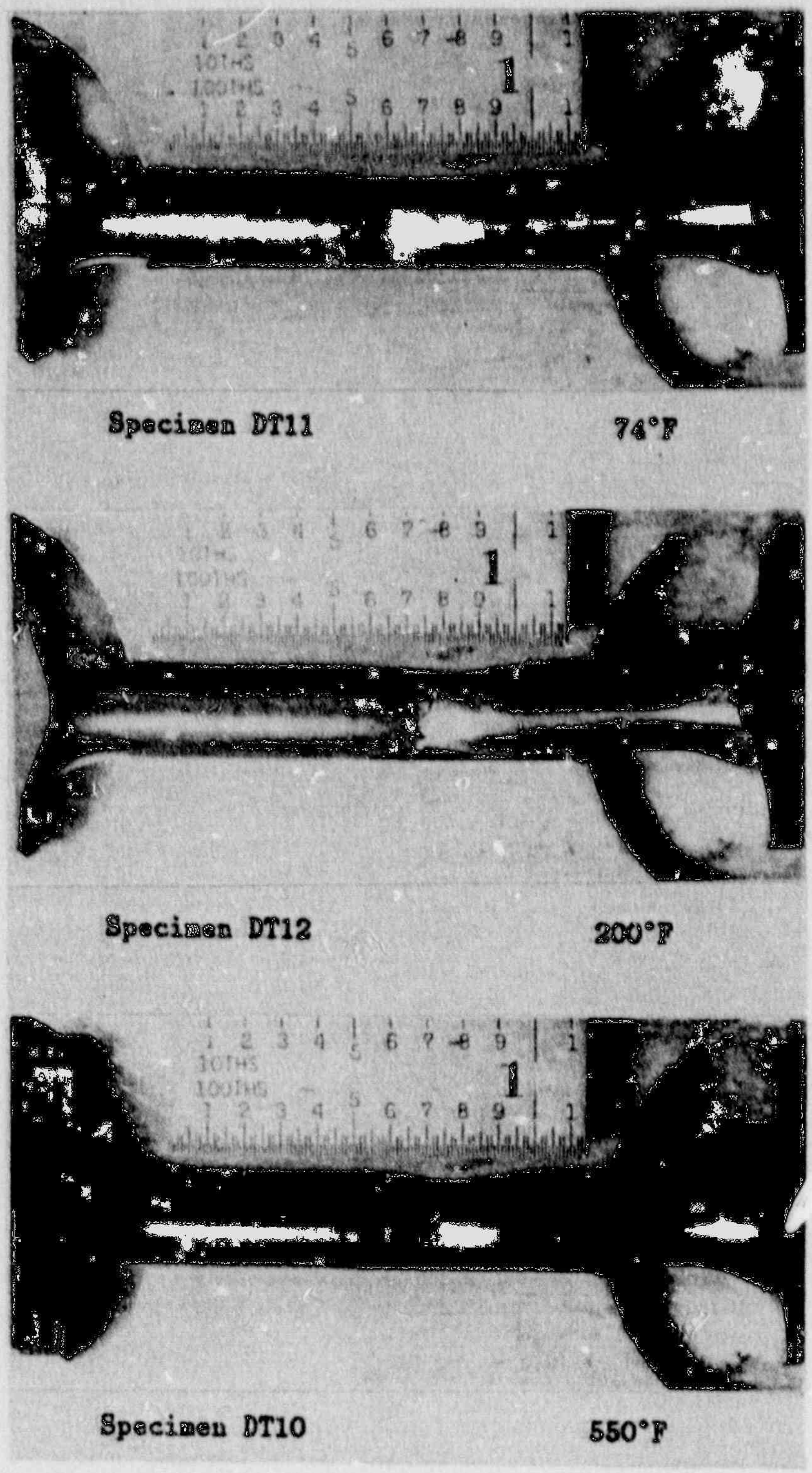

FIGURE 5-13 FRACTURED TENSILE SPECIMENS FOR MCGUIRE UNIT 1 REACTOR VESSEL SHELL PLATE B5012-1 (TRANSVERSE ORIENTATION)

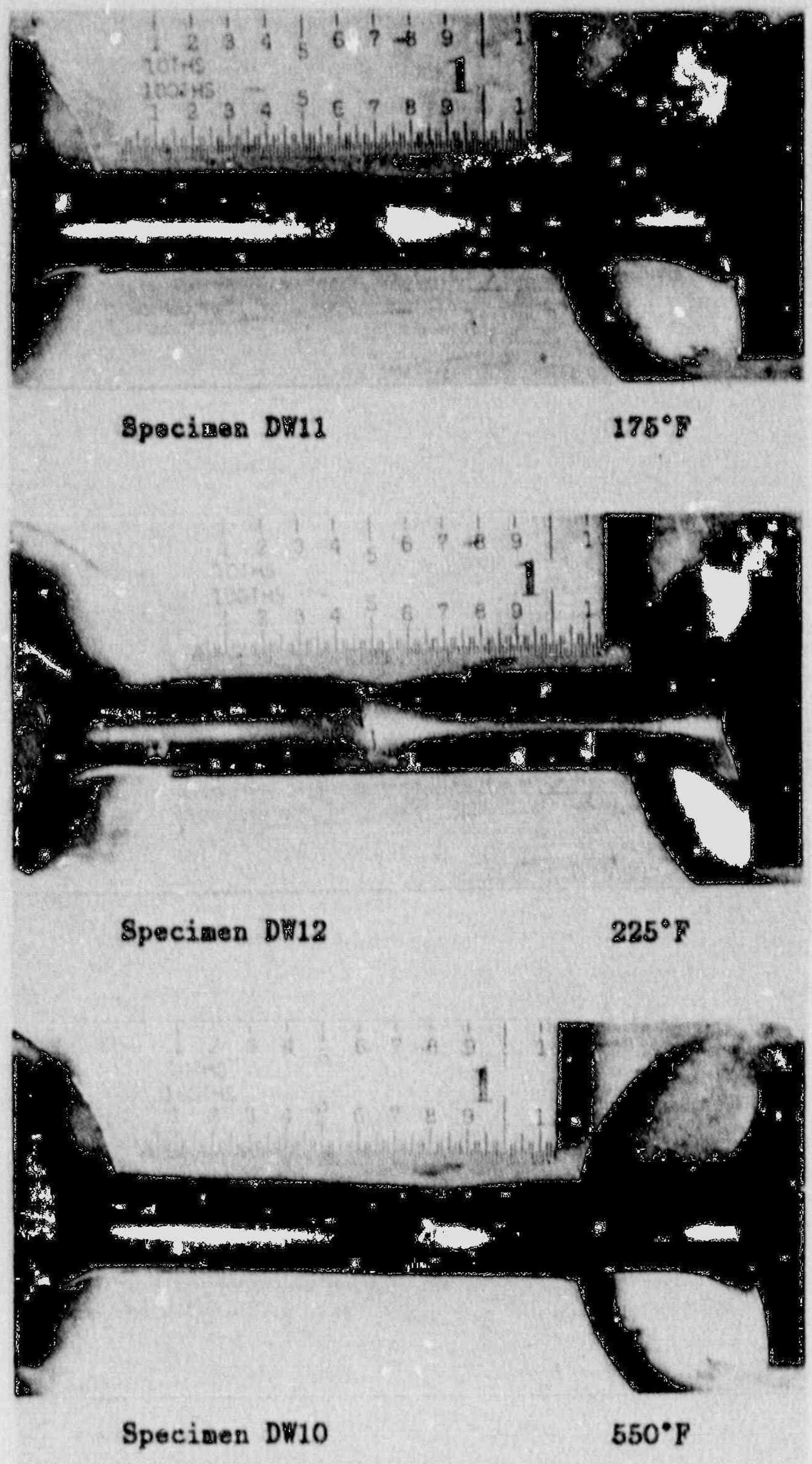

FIGURE 5-14 FRACTURED TENSILE SPECIMENS FOR MCGUIRE UNIT 1 REACTOR VESSEL WELD METAL

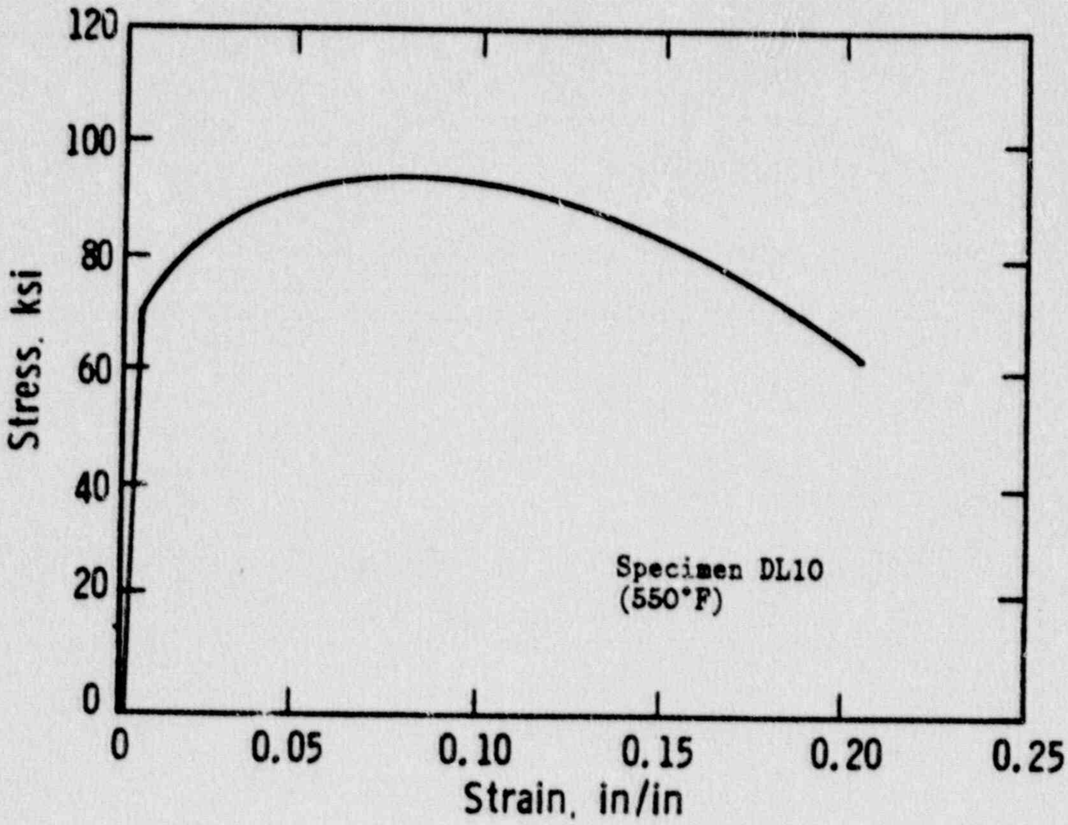

FIGURE 5-15 TYPICAL STRESS-STRAIN CURVE FOR TENSION SPECIMENS

3887s/081489:10

SECTION 6
RADIATION ANALYSIS AND NEUTRON DOSIMETRY

6.1 INTRODUCTION

Knowledge of the neutron environment within the reactor pressure vessel and surveillance capsule geometry is required as an integral part of LWR reactor pressure vessel surveillance programs for two reasons. First, in order to interpret the neutron radiation-induced material property changes observed in the test specimens, the neutron environment (energy spectrum, flux, fluence) to which the test specimens were exposed must be known. Second, in order to relate the changes observed in the test specimens to the present and future condition of the reactor vessel, a relationship must be established between the neutron environment at various positions within the reactor vessel and that experienced by the test specimens. The former requirement is normally met by employing a combination of rigorous analytical techniques and measurements obtained with passive neutron flux monitors contained in each of the surveillance capsules. The latter information is derived solely from analysis.

The use of fast neutron fluence ($E > 1.0$ MeV) to correlate measured materials properties changes to the neutron exposure of the material for light water reactor applications has traditionally been accepted for development of damage trend curves as well as for the implementation of trend curve data to assess vessel condition. In recent years, however, it has been suggested that an exposure model that accounts for differences in neutron energy spectra between surveillance capsule locations and positions within the vessel wall could lead to an improvement in the uncertainties associated with damage trend curves as well as to a more accurate evaluation of damage gradients through the pressure vessel wall.

Because of this potential shift away from a threshold fluence toward an energy dependent damage function for data correlation, ASTM Standard Practice E853, "Analysis and Interpretation of Light Water Reactor Surveillance Results," recommends reporting displacements per iron atom (dpa) along with fluence

(E > 1.0 MeV) to provide a data base for future reference. The energy dependent dpa function to be used for this evaluation is specified in ASTM Standard Practice E693, "Characterizing Neutron Exposures in Ferritic Steels in Terms of Displacements per Atom." The application of the dpa parameter to the assessment of embrittlement gradients through the thickness of the pressure vessel wall has already been promulgated in Revision 2 to the Regulatory Guide 1.99, "Radiation Embrittlement of Reactor Vessel Materials."

This section provides the results of the neutron dosimetry evaluations performed in conjunction with the analysis of test specimens contained in surveillance capsule X. Fast neutron exposure parameters in terms of fast neutron fluence (E > 1.0 MeV), fast neutron fluence (E > 0.1 Mev), and iron atom displacements (dpa) are established for the capsule irradiation history. The analytical formalism relating the measured capsule exposure to the exposure of the vessel wall is described and used to project the integrated exposure of the vessel itself. Also uncertainties associated with the derived exposure parameters at the surveillance capsule and with the projected exposure of the pressure vessel are provided.

6.2 DISCRETE ORDINATES ANALYSIS

A plan view of the reactor geometry at the core midplane is shown in Figure 4-1. Six irradiation capsules attached to the neutron pads are included in the reactor design to constitute the reactor vessel surveillance program. The capsules are located at azimuthal angles of 56°, 58.5°, 124°, 236°, 238.5°, and 304° relative to the core cardinal area as shown in Figure 4-1.

A plan view of a dual surveillance capsule holder attached to the neutron pad is shown in Figure 6-1. The stainless steel specimen containers are 1.182 by 1-inch and approximately 56 inches in height. The containers are positioned axially such that the specimens are centered on the core midplane, thus spanning the central 5 feet of the 12-foot high reactor core.

From a neutron transport standpoint, the surveillance capsule structures are significant. They have a marked effect on both the distribution of neutron flux and the neutron energy spectrum in the water annulus between the neutron pad and the reactor vessel. In order to properly determine the neutron environment at the test specimen locations, the capsules themselves must be included in the analytical model.

In performing the fast neutron exposure evaluations for the surveillance capsules and reactor vessel, two distinct sets of transport calculations were carried out. The first, a single computation in the conventional forward mode, was used primarily to obtain relative neutron energy distributions throughout the reactor geometry as well as to establish relative radial distributions of exposure parameters ($\phi(E > 1.0$ Mev,) $\phi(E > 0.1$ Mev), and dpa) through the vessel wall. The neutron spectral information was required for the interpretation of neutron dosimetry withdrawn from the surveillance capsule as well as for the determination of exposure parameter ratios; i.e., dpa/$\phi(E > 1.0$ MeV), within the pressure vessel geometry. The relative radial gradient information was required to permit the projection of measured exposure parameters to locations interior to the pressure vessel wall; i.e., the 1/4T, 1/2T, and 3/4T locations.

The second set of calculations consisted of a series of adjoint analyses relating the fast neutron flux ($E > 1.0$ MeV) at surveillance capsule positions, and several azimuthal locations on the pressure vessel inner radius to neutron source distributions within the reactor core. The importance functions generated from these adjoint analyses provided the basis for all absolute exposure projections and comparison with measurement. These importance functions, when combined with cycle specific neutron source distributions, yielded absolute predictions of neutron exposure at the locations of interest for the first 5 cycles of irradiation; and established the means to perform similar predictions and dosimetry evaluations for all subsequent fuel cycles. It is important to note that the cycle specific neutron source distributions utilized in these analyses included not only spatial variations of fission rates within the reactor core; but, also accounted for the effects of varying neutron yield per fission and fission spectrum introduced by the build-up of plutonium as the burnup of individual fuel assemblies increased.

The absolute cycle specific data from the adjoint evaluations together with relative neutron energy spectra and radial distribution information from the forward calculation provided the means to:

1. Evaluate neutron dosimetry obtained from surveillance capsule locations.

2. Extrapolate dosimetry results to key locations at the inner radius and through the thickness of the pressure vessel wall.

3. Enable a direct comparison of analytical prediction with measurement.

4. Establish a mechanism for projection of pressure vessel exposure as the design of each new fuel cycle evolves.

The forward transport calculation for the reactor model summarized in Figures 4-1 and 6-1 was carried out in R, θ geometry using the DOT two-dimensional discrete ordinates code [5] and the SAILOR cross-section library [6]. The SAILOR library is a 47 group ENDFB-IV based data set produced specifically for light water reactor applications. In these analyses anisotopic scattering was treated with a P_3 expansion of the cross-sections and the angular discretization was modeled with an S_8 order of angular quadrature.

The reference core power distribution utilized in the forward analysis was derived from statistical studies of long-term operation of Westinghouse 4-loop plants. Inherent in the development of this reference core power distribution is the use of an out-in fuel management strategy; i.e., fresh fuel on the core periphery. Furthermore, for the peripheral fuel assemblies, a 2σ uncertainty derived from the statistical evaluation of plant to plant and cycle to cycle variations in peripheral power was used. Since it is unlikely that a single reactor would have a power distribution at the nominal $+2\sigma$ level for a large number of fuel cycles, the use of this reference distribution is expected to yield somewhat conservative results.

All adjoint analyses were also carried out using an S_8 order of angular quadrature and the P_3 cross-section approximation from the SAILOR library. Adjoint source locations were chosen at several azimuthal locations along the pressure vessel inner radius as well as the geometric center of each surveillance capsule. Again, these calculations were run in R, Θ geometry to provide neutron source distribution importance functions for the exposure parameter of interest; in this case, ϕ (E > 1.0 MeV). Having the importance functions and appropriate core source distributions, the response of interest could be calculated as:

$$R(r, \theta) = \int_r \int_\theta \int_E I(r, \theta, E)\, S(r, \theta, E)\, r\, dr\, d\theta\, dE$$

where: $R(r, \theta)$ = ϕ (E > 1.0 MeV) at radius r and azimuthal angle Θ

$I(r, \theta, E)$ = Adjoint importance function at radius, r, azimuthal angle Θ, and neutron source energy E.

$S(r, \theta, E)$ = Neutron source strength at core location r, Θ and energy E.

Although the adjoint importance functions used in the McGuire Unit 1 analysis were based on a response function defined by the threshold neutron flux (E > 1.0 MeV), prior calculations have shown that, while the implementation of low leakage loading patterns significantly impact the magnitude and the spatial distribution of the neutron field, changes in the relative neutron energy spectrum are of second order. Thus, for a given location the ratio of dpa/ϕ (E > 1.0 MeV) is insensitive to changing core source distributions. In the application of these adjoint important functions to the McGuire Unit 1 reactor, therefore, calculation of the iron displacement rates (dpa) and the neutron flux (E > 0.1 MeV) were computed on a cycle specific basis by using dpa/ϕ (E > 1.0 MeV) and ϕ (E > 0.1 MeV)/ϕ (E > 1.0 MeV) ratios from the forward analysis in conjunction with the cycle specific ϕ (E > 1.0 MeV) solutions from the individual adjoint evaluations.

The reactor core power distribution used in the plant specific adjoint calculations was taken from the fuel cycle design report for the first five operating cycle of McGuire Unit 1 [7 thru 11]. The relative power levels in fuel assemblies that are significant contributors to the neutron exposure of the pressure vessel and surveillance capsules are summarized in Figure 6-2. For comparison purposes, the core power distribution (design basis) used in the reference forward calculation is also illustrated in Figure 6-2.

Selected results from the neutron transport analyses performed for the McGuire Unit 1 reactor are provided in Tables 6-1 through 6-5. The data listed in these tables establish the means for absolute comparisons of analysis and measurement for the capsule irradiation period and provide the means to correlate dosimetry results with the corresponding neutron exposure of the pressure vessel wall.

In Table 6-1, the calculated exposure parameters (ϕ (E > 1.0 MeV), ϕ (E > 0.1 MeV), and dpa) are given at the geometric center of the two surveillance capsule positions for both the design basis and the plant specific core power distributions. The plant specific data, based on the adjoint transport analysis, are meant to establish the absolute comparison of measurement with analysis. The design basis data derived from the forward calculation are provided as a point of reference against which plant specific fluence evaluations can be compared. Similar data is given in Table 6-2 for the pressure vessel inner radius. Again, the three pertinent exposure parameters are listed for both the design basis and the cycle 1 through 5 plant specific power distributions. It is important to note that the data for the vessel inner radius were taken at the clad/base metal interface; and, thus, represent the maximum exposure levels of the vessel wall itself.

Radial gradient information for neutron flux (E > 1.0 MeV), neutron flux (E > 0.1 MeV), and iron atom displacement rate is given in Tables 6-3, 6-4, and 6-5, respectively. The data, obtained from the forward neutron transport calculation, are presented on a relative basis for each exposure parameter at several azimuthal locations. Exposure parameter distributions within the wall may be obtained by normalizing the calculated or projected exposure at the vessel inner radius to the gradient data given in Tables 6-3 through 6-5.

For example, the neutron flux (E > 1.0 MeV) at the 1/4T position on the 45° aximuth is given by:

$$\phi_{1/4T}(45°) = \phi(220.27, 45°)\ F\ (225.75, 45°)$$

where $\phi_{1/4T}(45°)$ = Projected neutron flux at the 1/4T position on the 45° azimuth

ϕ (220.27, 45°) = Projected or calculated neutron flux at the vessel inner radius on the 45° azimuth.

F (225.75, 45°) = Relative radial distribution function from Table 6-3.

Similar expressions apply for exposure parameters in terms of ϕ(E > 0.1 MeV) and dpa/sec.

6.3 NEUTRON DOSIMETRY

The passive neutron sensors included in the McGuire Unit 1 surveillance program are listed in Table 6-6. Also given in Table 6-6 are the primary nuclear reactions and associated nuclear constants that were used in the evaluation of the neutron energy spectrum within the capsule and the subsequent determination of the various exposure parameters of interest (ϕ (E > 1.0 Mev), ϕ (E > 0.1 MeV), dpa).

The relative locations of the neutron sensors within the capsules are shown in Figure 4-2. The iron, nickel, copper, and cobalt-aluminum monitors, in wire form, were placed in holes drilled in spacers at several axial levels within the capsules. The cadmium-shielded neptunium and uranium fission monitors were accommodated within the dosimeter block located near the center of the capsule.

The use of passive monitors such as those listed in Table 6-6 does not yield a direct measure of the energy dependent flux level at the point of interest.

Rather, the activation or fission process is a measure of the integrated effect that the time- and energy-dependent neutron flux has on the target material over the course of the irradiation period. An accurate assessment of the average neutron flux level incident on the various monitors may be derived from the activation measurements only if the irradiation parameters are well known. In particular, the following variables are of interest:

- The specific activity of each monitor.
- The operating history of the reactor.
- The energy response of the monitor.
- The neutron energy spectrum at the monitor location.
- The physical characteristics of the monitor.

The specific activity of each of the neutron monitors was determined using established ASTM procedures [12 through 25]. Following sample preparation and weighing, the activity of each monitor was determined by means of a lithium-drifted germanium, Ge(Li), gamma spectrometer. The irradiation history of the McGuire Unit 1 reactor during cycles 1 through 5 was obtained from NUREG-0020, "Licensed Operating Reactors Status Summary Report" for the applicable period.

The irradiation history applicable to capsule X is given in Table 6-7. Measured and saturated reaction product specific activities as well as measured full power reaction rates are listed in Table 6-8. Reaction rate values were derived using the pertinent data from Tables 6-6 and 6-7.

Values of key fast neutron exposure parameters were derived from the measured reaction rates using the FERRET least squares adjustment code [26]. The FERRET approach used the measured reaction rate data and the calculated neutron energy spectrum at the the center of the surveillance capsule as input and proceeded to adjust a priori (calculated) group fluxes to produce a best fit (in a least squares sense) to the reaction rate data. The exposure parameters along with associated uncertainties where then obtained from the adjusted spectra.

In the FERRET evaluations, a log normal least-squares algorithm weights both the a priori values and the measured data in accordance with the assigned uncertainties and correlations. In general, the measured values f are linearly related to the flux ϕ by some response matrix A:

$$f_i^{(s,\alpha)} = \sum_g A_{ig}^{(s)} \phi_g^{(\alpha)}$$

where i indexes the measured values belonging to a single data set s, g designates the energy group and α delineates spectra that may be simultaneously adjusted. For example,

$$R_i = \sum_g \sigma_{ig} \phi_g$$

relates a set of measured reaction rates R_i to a single spectrum ϕ_g by the multigroup cross section σ_{ig}. (In this case, FERRET also adjusts the cross-sections.) The log normal approach automatically accounts for the physical constraint of positive fluxes, even with the large assigned uncertainties.

In the FERRET analysis of the dosimetry data, the continuous quantities (i.e., fluxes and cross-sections) were approximated in 53 groups. The calculated fluxes from the discrete ordinates analysis were expanded into the FERRET group structure using the SAND-II code [27]. This procedure was carried out by first expanding the a priori spectrum into the SAND-II 620 group structure using a SPLINE interpolation procedure for interpolation in regions where group boundaries do not coincide. The 620-point spectrum was then easily collapsed to the group scheme used in FERRET.

The cross-sections were also collapsed into the 53 energy-group structure using SAND II with calculated spectra (as expanded to 620 groups) as weighting functions. The cross sections were taken from the ENDF/B-V dosimetry file. Uncertainty estimates and 53 x 53 covariance matrices were constructed for each cross section. Correlations between cross sections were neglected due to data and code limitations, but are expected to be unimportant.

For each set of data or a priori values, the inverse of the corresponding relative covariance matrix M is used as a statistical weight. In some cases, as for the cross sections, a multigroup covariance matrix is used. More often, a simple parameterized form is used:

$$M_{gg'} = R_N^2 + R_g R_{g'} P_{gg'}$$

where R_N specifies an overall fractional normalization uncertainty (i.e., complete correlation) for the corresponding set of values. The fractional uncertainties R_g specify additional random uncertainties for group g that are correlated with a correlation matrix:

$$P_{gg'} = (1 - \theta)\, \delta_{gg'} + \theta \exp\left[-\frac{(g-g')^2}{2\gamma^2}\right]$$

The first term specifies purely random uncertainties while the second term describes short-range correlations over a range γ (θ specifies the strength of the latter term.)

For the a priori calculated fluxes, a short-range correlation of $\gamma = 6$ groups was used. This choice implies that neighboring groups are strongly correlated when θ is close to 1. Strong long-range correlations (or anticorrelations) were justified based on information presented by R. E. Maerker [28]. Maerker's results are closely duplicated when $\gamma = 6$. For the integral reaction rate covariances, simple normalization and random uncertainties were combined as deduced from experimental uncertainties.

Results of the FERRET evaluation of the capsule X dosimetry are given in Table 6-9 The data summarized in Table 6-9 indicated that the capsule received an integrated exposure of 1.38×10^{19} n/cm^2 (E > 1.0 MeV) with an associated uncertainty of $\pm$ 8%. Also reported are capsule exposures in terms of fluence (E > 0.1 MeV) and iron atom displacements (dpa). Summaries of the fit of the adjusted spectrum are provided in Table 6-10. In general, excellent results were achieved in the fits of the adjusted spectrum to the individual experimental reaction rates. The adjusted spectrum itself is tabulated in Table 6-11 for the FERRET 53 energy group structure.

A summary of the measured and calculated neutron exposure of capsule X is presented in Table 6-12. The agreement between calculation and measurement falls within $\pm$ 2-17% for all exposure parameters listed. The calculated fast neutron exposure (Φ (E > 1.0 MeV), Φ (E > 0.1 MeV), dpa) values agreed with the measurements to within 6-12% whereas, the thermal neutron fluence calculated for the exposure period was less than the measured value by 17 percent.

Neutron exposure projections at key locations on the pressure vessel inner radius are given in Table 6-13. Along with the current (4.33 EFPY) exposure derived from the capsule X measurements, projections are also provided for an exposure period of 16 EFPY and to end of vessel design life (32 EFPY). The time averaged exposure rates for the first 4.33 EFPY of operation were used to perform projections beyond the end of cycle 1 through 5 exposure period.

In the calculation of exposure gradients for use in the development of heatup and cooldown curves for the McGuire Unit 1 reactor coolant system, exposure projections to 16 EFPY and 32 EFPY were employed. Data based on both a fluence (E > 1.0 MeV) slope and a plant specific dpa slope through the vessel wall are provided in Table 6-14. In order to access RT_{NDT} vs. fluence trend curves, dpa equivalent fast neutron fluence levels for the 1/4T and 3/4T positions were defined by the relations

$$\Phi' \; 1/4T = \Phi \text{ (Surface) } \left(\frac{\text{dpa (1/4T)}}{\text{dpa (Surface)}} \right)$$

$$\Phi' \; 3/4T = \Phi \text{ (Surface) } \left(\frac{\text{dpa (3/4T)}}{\text{dpa (Surface)}} \right)$$

Using this approach results in the dpa equivalent fluence values listed in Table 6-14.

In Table 6-15 updated lead factors are listed for each of the McGuire Unit 1 surveillance capsules. These data may be used as a guide in establishing future withdrawal schedules for the remaining capsules.

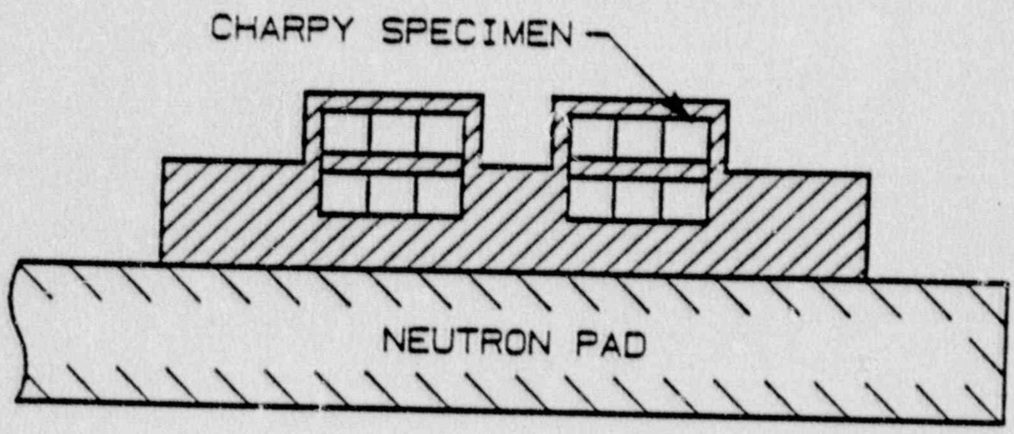

Figure 6-1. Plan View of a Dual Reactor Vessel Surveillance Capsule

1.01 0.72 1.03 0.77 0.84 0.87	1.04 0.75 1.05 0.77 0.71 0.72	0.96 0.67 0.97 0.67 0.81 0.77	0.77 0.55 0.77 0.51 0.50 0.39	DESIGN BASIS CYCLE 1 CYCLE 2 CYCLE 3 CYCLE 4 CYCLE 5	
1.02 0.99 0.93 0.92 0.91 1.03	1.10 1.05 1.30 1.22 1.20 1.19	1.00 0.95 0.93 0.93 1.00 1.06	1.05 0.97 1.25 1.15 1.12 1.10	1.10 0.80 1.07 0.76 0.69 0.69	0.71 0.49 0.69 0.45 0.41 0.35
1.05 1.14 0.79 1.17 1.09 1.13	0.87 1.10 0.8[illegible] 1.00 1.01 0.98	0.87 1.12 0.91 1.31 1.27 1.18	1.07 1.05 0.97 1.03 1.01 1.13	1.00 0.98 1.14 1.21 1.19 1.18	1.05 0.95 0.80 0.71 0.83 0.78
1.09 1.15 0.93 0.93 1.15 0.92	1.06 1.18 0.92 1.33 1.29 1.28	0.88 1.13 0.92 1.02 0.86 0.97	1.10 1.13 1.11 1.33 1.10 1.30	1.04 1.18 1.15 0.91 1.10 0.97	
0.90 1.19 0.90 1.28 1.09 1.10	1.04 1.15 0.94 1.00 1.11 1.13	1.12 1.19 1.15 1.33 1.28 1.31	0.92 1.14 1.11 1.01 1.13 0.96		

Figure 6-2. Core Power Distributions Used in Transport Calculations for McGuire Unit 1

TABLE 6-1

CALCULATED FAST NEUTRON EXPOSURE RATES AT THE SURVEILLANCE CAPSULE CENTER

	IRRADIATION TIME	ϕ (E > 1.0 Mev) $(n/cm^2\text{-sec})$		ϕ(E > 1.0 Mev) $(n/cm^2\text{-sec})$		dpa/sec	
CYCLE	(EFPS)	31.5°	34.0°	31.5°	34.0°	31.5°	34.0°
DESIGN BASIS		1.11×10^{11}	1.29×10^{11}	4.88×10^{11}	5.93×10^{11}	2.21×10^{-10}	2.62×10^{-10}
CYCLE 1	3.53×10^{7}	8.18×10^{10}	9.32×10^{10}	3.60×10^{11}	4.28×10^{11}	1.63×10^{-10}	1.89×10^{-10}
CYCLE 2	2.32×10^{7}	1.03×10^{11}	1.16×10^{11}	4.53×10^{11}	5.33×10^{11}	2.05×10^{-10}	2.36×10^{-10}
CYCLE 3	2.49×10^{7}	7.67×10^{10}	8.59×10^{10}	3.35×10^{11}	3.95×10^{11}	1.52×10^{-10}	1.74×10^{-10}
CYCLE 4	2.59×10^{7}	7.23×10^{10}	8.03×10^{10}	3.17×10^{11}	3.69×10^{11}	1.44×10^{-10}	1.63×10^{-10}
CYCLE 5	2.73×10^{7}	6.70×10^{10}	7.40×10^{10}	2.93×10^{11}	3.40×10^{11}	1.33×10^{-10}	1.50×10^{-10}

3887s/081489:10

TABLE 6-2

CALCULATED FAST NEUTRON EXPOSURE PARAMETERS AT
THE PRESSURE VESSEL CLAD/BASE METAL INTERFACE

ϕ (E > 1.0 Mev) (n/cm^2-sec)

	0°	15°	30°	45°
DESIGN BASIS	1.45×10^{10}	2.21×10^{10}	1.69×10^{10}	2.44×10^{10}
Cycle 1	1.07×10^{10}	1.60×10^{10}	1.24×10^{10}	1.75×10^{10}
Cycle 2	1.36×10^{10}	2.04×10^{10}	1.56×10^{10}	2.17×10^{10}
Cycle 3	1.07×10^{10}	1.56×10^{10}	1.17×10^{10}	1.61×10^{10}
Cycle 4	1.08×10^{10}	1.59×10^{10}	1.12×10^{10}	1.50×10^{10}
Cycle 5	1.08×10^{10}	1.52×10^{10}	1.03×10^{10}	1.38×10^{10}

ϕ (E > 0.1 Mev) (n/cm^2-sec)

	0°	15°	30°	45°
DESIGN BASIS	3.02×10^{10}	4.66×10^{10}	4.25×10^{10}	6.11×10^{10}
Cycle 1	2.23×10^{10}	3.37×10^{10}	3.12×10^{10}	4.38×10^{10}
Cycle 2	2.83×10^{10}	4.30×10^{10}	3.92×10^{10}	5.43×10^{10}
Cycle 3	2.29×10^{10}	3.29×10^{10}	2.94×10^{10}	4.03×10^{10}
Cycle 4	2.25×10^{10}	3.35×10^{10}	2.82×10^{10}	3.76×10^{10}
Cycle 5	2.25×10^{10}	3.21×10^{10}	2.59×10^{10}	3.46×10^{10}

dpa/sec

	0°	15°	30°	45°
DESIGN BASIS	2.25×10^{-11}	3.41×10^{-11}	2.73×10^{-11}	3.88×10^{-11}
Cycle 1	1.66×10^{-11}	2.47×10^{-11}	2.00×10^{-11}	2.78×10^{-11}
Cycle 2	2.11×10^{-11}	3.15×10^{-11}	2.52×10^{-11}	3.45×10^{-11}
Cycle 3	1.66×10^{-11}	2.41×10^{-11}	1.89×10^{-11}	2.56×10^{-11}
Cycle 4	1.68×10^{-11}	2.45×10^{-11}	1.80×10^{-11}	2.39×10^{-11}
Cycle 5	1.68×10^{-11}	2.35×10^{-11}	1.66×10^{-11}	2.19×10^{-11}

TABLE 6-3

RELATIVE RADIAL DISTRIBUTIONS OF NEUTRON FLUX (E > 1.0 MeV)
WITHIN THE PRESSURE VESSEL WALL

Radius (cm)	0°	15°	30°	45°
220.27[1]	1.00	1.00	1.00	1.00
220.64	0.979	0.979	0.980	0.979
221.66	0.891	0.891	0.893	0.889
222.99	0.771	0.769	0.773	0.766
224.31	0.655	0.652	0.658	0.648
225.63	0.552	0.549	0.555	0.543
226.95	0.463	0.459	0.467	0.452
228.28	0.387	0.383	0.390	0.376
229.60	0.322	0.318	0.326	0.311
230.92	0.268	0.263	0.271	0.257
232.25	0.222	0.218	0.225	0.211
233.57	0.183	0.180	0.187	0.174
234.89	0.151	0.148	0.155	0.142
236.22	0.125	0.121	0.128	0.116
237.54	0.102	0.0992	0.105	0.0945
238.86	0.0831	0.0807	0.0862	0.0762
240.19	0.0673	0.0650	0.0703	0.0608
241.51	0.0539	0.0512	0.0567	0.0472
242.17[2]	0.0508	0.0477	0.0536	0.04[illegible]

NOTES: 1) Base Metal Inner Radius
2) Base Metal Outer Radius

TABLE 6-4

RELATIVE RADIAL DISTRIBUTIONS OF NEUTRON FLUX (E > 0.1 MeV)
WITHIN THE PRESSURE VESSEL WALL

Radius (cm)	0°	15°	30°	45°
220.27(1)	1.00	1.00	1.00	1.00
220.64	1.00	1.00	1.00	1.00
221.66	1.00	1.00	1.00	0.995
222.99	0.974	0.966	0.982	0.956
224.31	0.928	0.915	0.938	0.902
225.63	0.875	0.859	0.886	0.843
226.95	0.819	0.802	0.832	0.782
228.28	0.762	0.743	0.777	0.722
229.60	0.705	0.686	0.721	0.663
230.92	0.649	0.629	0.665	0.605
232.25	0.594	0.575	0.611	0.549
233.57	0.540	0.522	0.558	0.495
234.89	0.488	0.470	0.506	0.443
236.22	0.436	0.421	0.455	0.392
237.54	0.386	0.373	0.406	0.343
238.86	0.337	0.326	0.358	0.296
240.19	0.290	0.280	0.310	0.248
241.51	0.244	0.232	0.261	0.201
242.17(2)	0.233	0.219	0.249	0.188

NOTES: 1) Base Metal Inner Radius
2) Base Metal Outer Radius

TABLE 6-5

RELATIVE RADIAL DISTRIBUTIONS OF IRON DISPLACEMENT RATE (dpa) WITHIN THE PRESSURE VESSEL WALL

Radius (cm)	0°	15°	30°	45°
220.27 (1)	1.00	1.00	1.00	1.00
220.64	0.982	0.982	0.986	0.984
221.66	0.911	0.910	0.923	0.915
222.99	0.813	0.812	0.837	0.821
224.31	0.721	0.718	0.751	0.730
225.63	0.637	0.633	0.673	0.646
226.95	0.562	0.558	0.602	0.572
228.28	0.496	0.491	0.539	0.505
229.60	0.438	0.433	0.481	0.447
230.92	0.387	0.381	0.430	0.394
232.25	0.341	0.335	0.383	0.347
233.57	0.300	0.295	0.341	0.305
234.89	0.263	0.258	0.302	0.266
236.22	0.230	0.225	0.267	0.231
237.54	0.199	0.195	0.234	0.199
238.86	0.171	0.168	0.203	0.169
240.19	0.145	0.142	0.174	0.140
241.51	0.121	0.117	0.146	0.113
242.17 (2)	0.116	0.110	0.140	0.106

NOTES: 1) Base Metal Inner Radius

2) Base Metal Outer Radius

TABLE 6-6

NUCLEAR PARAMETERS FOR NEUTRON FLUX MONITORS

Monitor Material	Reaction of Interest	Target Weight Fraction	Response Range	Product Half-Life	Fission Yield (%)
Copper	$Cu^{63}(n,\alpha)Co^{60}$	0.6917	E> 4.7 MeV	5.272 yrs	
Iron	$Fe^{54}(n,p)Mn^{54}$	0.0582	E> 1.0 MeV	312.2 days	
Nickel	$Ni^{58}(n,p)Co^{58}$	0.6830	E> 1.0 MeV	70.90 days	
Uranium-238*	$U^{238}(n,f)Cs^{137}$	1.0	E> 0.4 MeV	30.12 yrs	5.99
Neptunium-237*	$Np^{237}(n,f)Cs^{137}$	1.0	E> 0.08 MeV	30.12 yrs	6.50
Cobalt-Aluminum*	$Co^{59}(n,\gamma)Co^{60}$	0.0015	0.4ev<E< 0.015 MeV	5.272 yrs	
Cobalt-Aluminum	$Co^{59}(n,\gamma)Co^{60}$	0.0015	E< 0.015 MeV	5.272 yrs	

*Denotes that monitor is cadmium shielded.

TABLE 6-7

IRRADIATION HISTORY OF NEUTRON SENSORS CONTAINED IN CAPSULE X

Irradiation Period	P_j (MW_t)	$P_j/P_{Ref.}$	Irradiation Time (days)	Decay Time (days)
10/81	299	0.088	31	2671
11/81	1100	.322	30	2641
12/81	114	.034	31	2610
1/82	1712	.502	31	2579
2/82	1569	.460	28	2551
3/82	713	.209	31	2520
4/82	1656	.486	30	2490
5/82	1995	.585	31	2459
6/82	1758	.516	30	2429
7/82	755	.221	31	2398
8/82	1973	.578	31	2367
9/82	2020	.592	30	2337
10/82	2758	.809	31	2306
11/82	733	.215	30	2276
12/82	1996	.585	31	2245
1/83	1152	.338	31	2214
2/83	0	.000	28	2186
3/83	0	.000	31	2155
4/83	0	.000	30	2125
5/83	252	.074	31	2094
6/83	2714	.796	30	2064
7/83	265[illegible]	.778	31	2033
8/83	1518	.445	31	2002
9/83	3140	.921	30	1972
10/83	2601	.763	31	1941
11/83	2255	.661	30	1911
12/83	2704	.793	31	1880
1/84	2988	.876	31	1849
2/84	2715	.796	29	1820

TABLE 6-7 (Cont'd)

IRRADIATION HISTORY OF NEUTRON SENSORS
CONTAINED IN CAPSULE X

Irradiation Period	P_j (MW_t)	$P_j/P_{Ref.}$	Irradiation Time (days)	Decay Time (days)
3/84	0	.000	31	1789
4/84	0	.000	30	1759
5/84	2681	.786	31	1728
6/84	3148	.923	30	1698
7/84	3118	.914	31	1667
8/84	3186	.934	31	1636
9/84	3445	1.00	30	1606
10/84	2745	.805	31	1575
11/84	2157	.632	30	1545
12/84	305	.089	31	1514
1/85	3168	.929	31	1483
2/85	3108	.911	28	1455
3/85	2277	.668	31	1424
4/85	829	.243	30	1394
5/85	0	.000	31	1363
6/85	164	.048	30	1333
7/85	3151	.924	31	1302
8/85	3405	.998	31	1271
9/85	3236	.949	30	1241
10/85	3406	.999	31	1210
11/85	2139	.627	30	1180
12/85	3260	.956	31	1149
1/86	3322	.974	31	1118
2/86	3010	.882	28	1090
3/86	2808	.823	31	1059
4/86	3062	.898	30	1029
5/86	1346	.395	31	998
6/86	0	.000	30	968
7/86	0	.000	31	937

TABLE 6-7 (Cont'd)

IRRADIATION HISTORY OF NEUTRON SENSORS
CONTAINED IN CAPSULE X

Irradiation Period	P_j (MW_t)	$P_j/P_{Ref.}$	Irradiation Time (days)	Decay Time (days)
8/86	0	.000	31	906
9/86	1311	.385	30	876
10/86	3082	.904	31	845
11/86	62	.018	30	815
12/86	3383	.992	31	784
1/87	3407	.999	31	753
2/87	2769	.812	28	725
3/87	3411	1.00	31	694
4/87	3177	.931	30	664
5/87	3354	.983	31	633
6/87	3391	.994	30	603
7/87	3407	.999	31	572
8/87	2484	.728	31	541
9/87	308	.090	30	511
10/87	0	.000	31	480
11/87	1530	.449	30	450
12/87	3026	.887	31	419
1/88	3199	.938	31	388
2/88	3326	.975	29	359
3/88	3200	.938	31	328
4/88	3215	.943	30	298
5/88	3399	.997	31	267
6/88	3168	.929	30	237
7/88	3341	.979	31	206
8/88	3390	.994	31	175
9/88	3386	.993	30	145
10/88	3119	.914	12	133

NOTE: Reference Power = 3411 MW_t

TABLE 6-8

MEASURED SENSOR ACTIVITIES AND REACTION RATES

Monitor and Axial Location	Measured Activity (dis/sec-gm)	Saturated Activity (dis/sec-gm)	Reaction Rate (RPS/NUCLEUS)
Cu-63 (n,α) Co-60			
Top	1.26×10^5	3.44×10^5	
Middle	1.25×10^5	3.41×10^5	
Bottom	1.29×10^5	3.52×10^5	
Average	1.27×10^5	3.46×10^5	5.28×10^{-17}
Fe-54(n,p) Mn-54			
Top	1.65×10^6	3.22×10^6	
Middle	1.64×10^6	3.20×10^6	
Bottom	1.73×10^6	3.37×10^6	
Average	1.67×10^6	3.26×10^6	5.20×10^{-15}
Ni-58 (n,p) Co-58			
Top	1.10×10^7	5.15×10^7	
Middle	1.07×10^7	5.01×10^7	
Bottom	1.12×10^7	5.24×10^7	
Average	1.10×10^7	5.13×10^7	7.33×10^{-15}
U-238 (n,f) Cs-137 (Cd)			
Middle	5.33×10^5	5.81×10^6	3.83×10^{-14}

TABLE 6-8

MEASURED SENSOR ACTIVITIES AND REACTION RATES - cont'd

Monitor and Axial Location	Measured Activity (dis/sec-gm)	Saturated Activity (dis/sec-gm)	Reaction Rate (RPS/NUCLEUS)
Np-237(n,f) Cs-137 (Cd)			
Middle	3.91×10^{6}	4.26×10^{7}	2.58×10^{-13}
Co-59 (n,γ) Co-60			
Top	3.14×10^{7}	8.57×10^{7}	
Middle	3.35×10^{7}	9.14×10^{7}	
Bottom	3.00×10^{7}	8.19×10^{7}	
Average	3.16×10^{7}	8.63×10^{7}	5.63×10^{-12}
Co-59 (n,γ) Co-60 (Cd)			
Top	1.68×10^{7}	4.59×10^{7}	
Middle	1.68×10^{7}	4.59×10^{7}	
Bottom	1.55×10^{7}	4.23×10^{7}	
Average	1.64×10^{7}	4.47×10^{7}	2.91×10^{-12}

TABLE 6-9

SUMMARY OF NEUTRON DOSIMETRY RESULTS

	TIME AVERAGED EXPOSURE RATES	
ϕ (E> 1.0 MeV) (n/cm^2-sec)	1.01×10^{11}	$\pm$ 8%
ϕ (E> 0.1 MeV) (n/cm^2-sec)	4.26×10^{11}	$\pm$ 15%
dpa/sec	1.89×10^{-10}	$\pm$ 11%
ϕ(E< 0.414 eV) (n/cm^2-sec)	4.22×10^{10}	$\pm$ 29%
	INTEGRATED CAPSULE EXPOSURE	
Φ (E> 1.0 MeV) (n/cm^2)	1.38×10^{19}	$\pm$ 8%
Φ (E> 0.1 MeV) (n/cm^2)	5.82×10^{19}	$\pm$ 15%
dpa	2.58×10^{-2}	$\pm$ 11%
Φ (E< 0.414 eV) (n/cm^2)	5.77×10^{18}	$\pm$ 29%

NOTE: Total Irradiation Time = 4.33 EFPY

TABLE 6-10

COMPARISON OF MEASURED AND FERRET CALCULATED
REACTION RATES AT THE SURVEILLANCE CAPSULE CENTER

Reaction	Measured	Adjusted Calculation	C/M
Cu-63 (n,α) Co-60	5.28×10^{-17}	5.26×10^{-17}	1.00
Fe-54 (n,p) Mn-54	5.20×10^{-15}	5.34×10^{-15}	1.03
Ni-58 (n,p) Co-58	7.33×10^{-15}	7.35×10^{-15}	1.00
U-238 (n,f) Cs-137 (Cd)	3.83×10^{-14}	3.20×10^{-14}	0.83
Np-237 (n,f) Cs-137 (Cd)	2.58×10^{-13}	2.88×10^{-13}	1.12
Co-59 (n,γ) Co-60 (Cd)	2.91×10^{-12}	2.91×10^{-12}	1.00
Co-59 (n,γ) Co-60	5.63×10^{-12}	5.62×10^{-12}	1.00

TABLE 6-11

ADJUSTED NEUTRON ENERGY SPECTRUM AT
THE SURVEILLANCE CAPSULE CENTER

Group	Energy (Mev)	Adjusted Flux (n/cm^2-sec)	Group	Energy (Mev)	Adjusted Flux (n/cm^2-sec)
1	$1.73x10^{1}$	$4.23x10^{6}$	28	$9.12x10^{-3}$	$1.98x10^{10}$
2	$1.49x10^{1}$	$1.04x10^{7}$	29	$5.53x10^{-3}$	$2.60x10^{10}$
3	$1.35x10^{1}$	$4.83x10^{7}$	30	$3.36x10^{-3}$	$8.24x10^{9}$
4	$1.16x10^{1}$	$1.24x10^{8}$	31	$2.84x10^{-3}$	$7.98x10^{9}$
5	$1.00x10^{1}$	$3.02x10^{8}$	32	$2.40x10^{-3}$	$7.77x10^{9}$
6	$8.61x10^{0}$	$5.50x10^{8}$	33	$2.04x10^{-3}$	$2.20x10^{10}$
7	$7.41x10^{0}$	$1.32x10^{9}$	34	$1.23x10^{-3}$	$2.04x10^{10}$
8	$6.07x10^{0}$	$1.92x10^{9}$	35	$7.49x10^{-4}$	$1.90x10^{10}$
9	$4.97x10^{0}$	$4.07x10^{9}$	36	$4.54x10^{-4}$	$1.82x10^{10}$
10	$3.68x10^{0}$	$5.43x10^{9}$	37	$2.75x10^{-4}$	$1.96x10^{10}$
11	$2.87x10^{0}$	$1.14x10^{10}$	38	$1.67x10^{-4}$	$2.24x10^{10}$
12	$2.23x10^{0}$	$1.57x10^{10}$	39	$1.01x10^{-4}$	$2.12x10^{10}$
13	$1.74x10^{0}$	$2.19x10^{10}$	40	$6.14x10^{-5}$	$2.06x10^{10}$
14	$1.35x10^{0}$	$2.37x10^{10}$	41	$3.73x10^{-5}$	$2.00x10^{10}$
15	$1.11x10^{0}$	$4.28x10^{10}$	42	$2.26x10^{-5}$	$1.91x10^{10}$
16	$8.21x10^{-1}$	$4.84x10^{10}$	43	$1.37x10^{-5}$	$1.83x10^{10}$
17	$6.39x10^{-1}$	$5.00x10^{10}$	44	$8.32x10^{-6}$	$1.72x10^{10}$
18	$4.98x10^{-1}$	$3.61x10^{10}$	45	$5.04x10^{-6}$	$1.55x10^{10}$
19	$3.88x10^{-1}$	$5.15x10^{10}$	46	$3.06x10^{-6}$	$1.42x10^{10}$
20	$3.02x10^{-1}$	$5.11x10^{10}$	47	$1.86x10^{-6}$	$1.28x10^{10}$
21	$1.83x10^{-1}$	$5.12x10^{10}$	48	$1.13x10^{-6}$	$9.56x10^{9}$
22	$1.11x10^{-1}$	$4.11x10^{10}$	49	$6.83x10^{-7}$	$9.97x10^{9}$
23	$6.74x10^{-2}$	$2.85x10^{10}$	50	$4.14x10^{-7}$	$1.11x10^{10}$
24	$4.09x10^{-2}$	$1.62x10^{10}$	51	$2.51x10^{-7}$	$9.09x10^{9}$
25	$2.55x10^{-2}$	$2.23x10^{10}$	52	$1.52x10^{-7}$	$7.28x10^{9}$
26	$1.99x10^{-2}$	$1.07x10^{10}$	53	$9.24x10^{-8}$	$1.47x10^{10}$
27	$1.50x10^{-2}$	$1.35x10^{10}$			

NOTE: Tabulated energy levels represent the upper energy of each group.

TABLE 6-12

COMPARISON OF CALCULATED AND MEASURED EXPOSURE LEVELS FOR CAPSULE X

	Calculated	Measured	C/M
Φ(E> 1.0 MeV) (n/cm^2)	1.22×10^{19}	1.38×10^{19}	0.88
Φ(E> 0.1 MeV) (n/cm^2)	5.73×10^{19}	5.82×10^{19}	0.98
dpa	2.43×10^{-2}	2.58×10^{-2}	0.94
Φ(E< 0.414 eV) (n/cm^2)	4.81×10^{18}	5.77×10^{18}	0.83

TABLE 6-13
NEUTRON EXPOSURE PROJECTIONS AT KEY LOCATIONS
ON THE PRESSURE VESSEL CLAD/BASE METAL INTERFACE

	AZIMUTHAL ANGLE			
	0°	15°	30°	45°
4.33 EFPY				
Φ(E> 1.0 MeV) (n/cm^2)	1.74×10^{18}	2.57×10^{18}	1.89×10^{18}	2.60×10^{18}
Φ(E> 0.1 MeV) (n/cm^2)	3.25×10^{18}	4.87×10^{18}	4.27×10^{18}	5.85×10^{18}
dpa	2.53×10^{-3}	3.71×10^{-3}	2.86×10^{-3}	3.87×10^{-3}
16.0 EFPY				
Φ(E> 1.0 MeV) (n/cm^2)	6.43×10^{18}	9.50×10^{18}	6.98×10^{18}	9.61×10^{18}
Φ(E> 0.1 MeV) (n/cm^2)	1.20×10^{19}	1.80×10^{19}	1.58×10^{19}	2.16×10^{19}
dpa	9.35×10^{-3}	1.37×10^{-2}	1.06×10^{-2}	1.43×10^{-2}
32.0 EFPY				
Φ(E> 1.0 MeV) (n/cm^2)	1.29×10^{19}	1.90×10^{19}	1.40×10^{19}	1.92×10^{19}
Φ(E> 0.1 MeV) (n/cm^2)	2.40×10^{19}	3.60×10^{19}	3.16×10^{19}	4.32×10^{19}
dpa	1.87×10^{-2}	2.74×10^{-2}	2.11×10^{-2}	2.86×10^{-2}

TABLE 6-14

NEUTRON EXPOSURE VALUES FOR USE IN THE GENERATION OF HEATUP/COOLDOWN CURVES

16 EFPY

	NEUTRON FLUENCE (E > 1.0 MeV) SLOPE (n/cm^2)			dpa SLOPE (equivalent n/cm^2)		
	Surface	1/4 T	3/4 T	Surface	1/4 T	3/4 T
0°	6.43×10^{18}	3.50×10^{18}	7.50×10^{17}	6.43×10^{18}	4.05×10^{18}	1.41×10^{18}
15°	9.50×10^{18}	5.14×10^{18}	1.07×10^{18}	9.50×10^{18}	5.95×10^{18}	2.03×10^{18}
30°	6.98×10^{18}	3.82×10^{18}	8.35×10^{17}	6.98×01^{18}	4.65×10^{18}	1.78×10^{18}
45°	9.61×10^{18}	5.14×10^{18}	1.04×10^{18}	9.61×10^{18}	6.14×10^{18}	2.11×10^{18}

32 EFPY

	NEUTRON FLUENCE (E > 1.0 MeV) SLOPE (n/cm^2)			dpa SLOPE (equivalent n/cm^2)		
	Surface	1/4 T	3/4 T	Surface	1/4 T	3/4 T
0°	1.29×10^{19}	7.02×10^{18}	1.50×10^{18}	1.29×10^{19}	8.10×10^{18}	2.82×10^{18}
15°	1.90×10^{19}	1.03×10^{19}	2.14×10^{18}	1.90×10^{19}	1.19×10^{19}	4.06×10^{18}
30°	1.40×10^{19}	7.66×10^{18}	1.67×10^{18}	1.40×01^{19}	9.30×10^{18}	3.56×10^{18}
45°	1.92×10^{19}	1.03×10^{19}	2.08×10^{18}	1.92×10^{19}	1.23×10^{19}	4.22×10^{18}

3897s/081489:10

TABLE 6-15

UPDATED LEAD FACTORS FOR McGUIRE UNIT 1 SURVEILLANCE CAPSULES

Capsule	Lead Factor
U	5.33[a]
X	5.31[a]
W	5.31
Z	5.31
V	4.76
Y	4.76

(a) Plant specific evaluation

SECTION 7
SURVEILLANCE CAPSULE REMOVAL SCHEDULE

The following removal schedule meets ASTM E185-82 and is recommended for future capsules to be removed from the McGuire Unit 1 reactor vessel:

Capsule	Vessel Location (deg)	Lead Factor	Removal Time(a)	Estimated Capsule Fluence (n/cm^2)
U	56	5.33	1.06	4.14×10^{18} (b)
X	236	5.31	4.33	1.38×10^{19} (b)
V	58.5	4.76	7	2.00×10^{19} (c)
Y	238.5	4.76	10	2.86×10^{19}
W	124	5.31	Standby	--
Z	304	5.31	Standby	--

a) Effective full power years from plant startup

b) Actual fluence

c) Approximate fluence at vessel inner wall at end of life (32 EFPY)

SECTION 8
REFERENCES

1. Davidson, J.A., and Yanichko, S.E., "Duke Power Company William B. McGuire Unit No. 1 Reactor Vessel Radiation Surveillance Program," WCAP-9195, November 1977.

2. Yanichko, S.E., et al., "Analysis of Capsule U from the Duke Power Company McGuire Unit 1 Reactor Vessel Radiation Surveillance Program, WCAP-10786, February 1985.

3. Code of Federal Regulations, 10CFR50, Appendix G, "Fracture Toughness Requirements" and Appendix H, "Reactor Vessel Material Surveillance Program Requirements", U. S. Nuclear Regulatory Commission, Washington, D.C.

4. Regulatory Guide 1.99, Revision 2, "Radiation Embrittlement of Reactor Vessel Materials," U.S. Nuclear Regulatory Commission, May, 1988.

5. R. G. Soltesz, R. K. Disney, J. Jedruch, and S. L. Ziegler, "Nuclear Rocket Shielding Methods, Modification, Updating and Input Data Preparation. Vol. 5--Two-Dimensional Discrete Ordinates Transport Technique", WANL-PR(LL)-034, Vol. 5, August 1970.

6. "ORNL RSCI Data Library Collection DLC-76, SAILOR Coupled Self-Shielded, 47 Neutron, 20 Gamma-Ray, P3, Cross Section Library for Light Water Reactors".

7. A. Saeed, et al., "The Nuclear Design and Core Physics Characteristics of the W. B. McGuire Unit 1 Nuclear Power Plant - Cycle 1, "WCAP-9323, May 1978. (Proprietary)

8. J. R. Lesko, et al., "The Nuclear Design and Core Physics Characteristics of the McGuire Unit 1 Nuclear Power Plant - Cycle 2," WCAP-10463, January 1984. (Proprietary)

9. J. R. Lesko, et al., "The Nuclear Design and Core Physics Characteristics of the McGuire Unit 1 Nuclear Power Plant - Cycle 3," WCAP-10782, February 1985. (Proprietary)

10. J. R. Lesko, et al., "The Nuclear Design and Core Physics Characteristics of the McGuire Unit 1 Nuclear Power Plant - Cycle 4," WCAP-11141, May 1986. (Proprietary)

11. J. R. Lesko, et al., "The Nuclear Design and Core Physics Characteristics of the McGuire Unit 1 Nuclear Power Plant - Cycle 5," WCAP-11589, October 1987. (Proprietary)

12. ASTM Designation E482-82, "Standard Guide for Application of Neutron Transport Methods for Reactor Vessel Surveillance", in ASTM Standards, Section 12, American Society for Testing and Materials, Philadelphia, PA, 1984.

13. ASTM Designation E560-77, "Standard Recommended Practice for Extrapolating Reactor Vessel Surveillance Dosimetry Results", in ASTM Standards, Section 12, American Society for Testing and Materials, Philadelphia, PA, 1984.

14. ASTM Designation E693-79, "Standard Practice for Characterizing Neutron Exposures in Ferritic Steels in Terms of Displacements per Atom (dpa)", in ASTM Standards, Section 12, American Society for Testing and Materials, Philadelphia, PA, 1984.

15. ASTM Designation E706-81a, "Standard Master Matrix for Light-Water Reactor Pressure Vessel Surveillance Standard", in ASTM Standards, Section 12, American Society for Testing and Materials, Philadelphia, PA, 1984.

16. ASTM Designation E853-84, "Standard Practice for Analysis and Interpretation of Light-Water Reactor Surveillance Results", in ASTM Standards, Section 12, American Society for Testing and Materials, Philadelphia, PA, 1984.

17. ASTM Designation E261-77, "Standard Method for Determining Neutron Flux, Fluence, and Spectra by Radioactivation Techniques", in ASTM Standards, Section 12, American Society for Testing and Materials, Philadelphia, PA, 1984.

18. ASTM Designation E262-77, "Standard Method for Measuring Thermal Neutron Flux by Radioactivation Techniques", in ASTM Standards, Section 12, American Society for Testing and Materials, Philadelphia, PA, 1984.

19. ASTM Designation E263-82, "Standard Method for Determining Fast-Neutron Flux Density by Radioactivation of Iron", in ASTM Standards, Section 12, American Society for Testing and Materials, Philadelphia, PA, 1984.

20. ASTM Designation E264-82, "Standard Method for Determining Fast-Neutron Flux Density by Radioactivation of Nickel", in ASTM Standards, Section 12, American Society for Testing and Materials, Philadelphia, PA, 1984.

21. ASTM Designation E481-78, "Standard Method for Measuring Neutron-Flux Density by Radioactivation of Cobalt and Silver", in ASTM Standards, Section 12, American Society for Testing and Materials, Philadelphia, PA, 1984.

22. ASTM Designation E523-82, "Standard Method for Determining Fast-Neutron Flux Density by Radioactivation of Copper", in ASTM Standards, Section 12, American Society for Testing and Materials, Philadelphia, PA, 1984.

23. ASTM Designation E704-84, "Standard Method for Measuring Reaction Rates by Radioactivation of Uranium-238", in ASTM Standards, Section 12, American Society for Testing and Materials, Philadelphia, PA, 1984.

24. ASTM Designation E705-79, "Standard Method for Measuring Fast-Neutron Flux Density by Radioactivation of Neptunium-237", in ASTM Standards, Section 12, American Society for Testing and Materials, Philadelphia, PA, 1984.

25. ASTM Designation E1005-84, "Standard Method for Application and Analysis of Radiometric Monitors for Reactor Vessel Surveillance", in ASTM Standards, Section 12, American Society for Testing and Materials, Philadelphia, PA, 1984.

26. F. A. Schmittroth, FERRET Data Analysis Core, HEDL-TME 79-40, Hanford Engineering Development Laboratory, Richland, WA, September 1979.

27. W. N. McElroy, S. Berg and T. Crocket, A Computer-Automated Iterative Method of Neutron Flux Spectra Determined by Foil Activation, AFWL-TR-67-41, Vol. I-IV, Air Force Weapons Laboratory, Kirkland AFB, NM, July 1967.

28. EPRI-NP-2188, "Development and Demonstration of an Advanced Methodology for LWR Dosimetry Applications", R. E. Maerker, et al., 1981.

APPENDIX A
HEATUP AND COOLDOWN LIMIT CURVES
FOR NORMAL OPERATION

A-1. INTRODUCTION

Heatup and cooldown limit curves are calculated using the most limiting value of RT_{NDT} (reference nil-ductility temperature) for the reactor vessel. The most limiting RT_{NDT} of the material in the core region of the reactor vessel is determined by using the preservice reactor vessel material fracture toughness properties and estimating the radiation-induced ΔRT_{NDT}. RT_{NDT} is designated as the higher of either the drop weight nil-ductility transition temperature (NDTT) or the temperature at which the material exhibits at least 50 ft-lb of impact energy and 35-mil lateral expansion (normal to the major working direction) minus 60°F.

RT_{NDT} increases as the material is exposed to fast-neutron radiation. Therefore, to find the most limiting RT_{NDT} at any time period in the reactor's life, ΔRT_{NDT} due to the radiation exposure associated with that time period must be added to the original unirradiated RT_{NDT}. The extent of the shift in RT_{NDT} is enhanced by certain chemical elements (such as copper and nickel) present in reactor vessel steels. The Nuclear Regulatory Commission (NRC) has published a method for predicting radiation embrittlement in Regulatory Guide 1.99 Rev. 2 (Radiation Embrittlement of Reactor Vessel Materials)[A-1]. The value, "f", given in figure A-1 is the calculated value of the neutron fluence at the location of interest (inner surface, 1/4T, or 3/4T) in the vessel at the location of the postulated defect, n/cm^2 (E > 1 MeV) divided by 10^{19}. The fluence factor is determined from figure A-1.

A-2. FRACTURE TOUGHNESS PROPERTIES

The fracture-toughness properties of the ferritic material in the reactor coolant pressure boundary are determined in accordance with the NRC Regulatory Standard Review Plan[A-2]. The pre-irradiation fracture-toughness properties of McGuire Unit 1 of the reactor vessels are presented in table A-1.

A-3. CRITERIA FOR ALLOWABLE PRESSURE-TEMPERATURE RELATIONSHIPS

The ASME approach for calculating the allowable limit curves for various heatup and cooldown rates specifies that the total stress intensity factor, K_I, for the combined thermal and pressure stresses at any time during heatup or cooldown cannot be greater than the reference stress intensity factor, K_{IR}, for the metal temperature at that time. K_{IR} is obtained from the reference fracture toughness curve, defined in Appendix G to the ASME Code[A-3]. The K_{IR} curve is given by the following equation:

$$K_{IR} = 26.78 + 1.223 \exp [0.0145 (T-RT_{NDT} + 160)] \qquad (1)$$

where

K_{IR} = reference stress intensity factor as a function of the metal temperature T and the metal reference nil-ductility temperature RT_{NDT}

Therefore, the governing equation for the heatup-cooldown analysis is defined in Appendix G of the ASME Code[A-3] as follows:

$$C\, K_{IM} + K_{IT} \leq K_{IR} \qquad (2)$$

where

K_{IM} = stress intensity factor caused by membrane (pressure) stress

K_{IT} = stress intensity factor caused by the thermal gradients

K_{IR} = function of temperature relative to the RT_{NDT} of the material

C = 2.0 for Level A and Level B service limits

C = 1.5 for hydrostatic and leak test conditions during which the reactor core is not critical

At any time during the heatup or cooldown transient, K_{IR} is determined by the metal temperature at the tip of the postulated flaw, the appropriate value for RT_{NDT}, and the reference fracture toughness curve. The thermal stresses resulting from the temperature gradients through the vessel wall are calculated and then the corresponding (thermal) stress intensity factors, K_{IT}, for the reference flaw are computed. From equation 2, the pressure stress intensity factors are obtained and, from these, the allowable pressures are calculated.

For the calculation of the allowable pressure versus coolant temperature during cooldown, the reference flaw of Appendix G to the ASME Code is assumed to exist at the inside of the vessel wall. During cooldown, the controlling location of the flaw is always at the inside of the wall because the thermal gradients produce tensile stresses at the inside, which increase with increasing cooldown rates. Allowable pressure-temperature relations are generated for both steady-state and finite cooldown rate situations. From these relations, composite limit curves are constructed for each cooldown rate of interest.

The use of the composite curve in the cooldown analysis is necessary because control of the cooldown procedure is based on the measurement of reactor coolant temperature, whereas the limiting pressure is actually dependent on the material temperature at the tip of the assumed flaw.

During cooldown, the 1/4 T vessel location is at a higher temperature than the fluid adjacent to the vessel ID. This condition, of course, is not true for the steady-state situation. It follows that, at any given reactor coolant temperature, the ΔT developed during cooldown results in a higher value of K_{IR} at the 1/4 T location for finite cooldown rates than for steady-state operation. Furthermore, if conditions exist so that the increase in K_{IR} exceeds K_{IT}, the calculated allowable pressure during cooldown will be greater than the steady-state value.

The above procedures are needed because there is no direct control on temperature at the 1/4 T location and, therefore, allowable pressures may unknowingly be violated if the rate of cooling is decreased at various intervals along a cooldown ramp. The use of the composite curve eliminates this problem and ensures conservative operation of the system for the entire cooldown period.

Three separate calculations are required to determine the limit curves for finite heatup rates. As is done in the cooldown analysis, allowable pressure-temperature relationships are developed for steady-state conditions as well as finite heatup rate conditions assuming the presence of a 1/4 T defect at the inside of the wall that alleviate the tensile stresses produced by internal pressure. The metal temperature at the crack tip lags the coolant temperature; therefore, the K_{IR} for the 1/4 T crack during heatup is lower than the K_{IR} for the 1/4 T crack during steady-state conditions at the same time coolant temperature. During heatup, especially at the end of the transient, conditions may exist so that the effects of compressive thermal stresses and lower K_{IR}'s do not offset each other, and the pressure-temperature curve based on steady-state conditions no longer represents a lower bound of all similar curves for finite heatup rates when the 1/4 T flaw is considered. Therefore, both cases have to be analyzed in order to ensure that at any coolant temperature the lower value of the allowable pressure calculated for steady-state and finite heatup rates is obtained.

The second portion of the heatup analysis concerns the calculation of the pressure-temperature limitations for the case in which a 1/4 T deep outside surface flaw is assumed. Unlike the situation at the vessel inside surface, the thermal gradients established at the outside surface during heatup produce stresses which are tensile in nature and therefore tend to reinforce any pressure stresses present. These thermal stresses are dependent on both the rate of heatup and the time (or coolant temperature) along the heatup ramp. Since the thermal stresses at the outside are tensile and increase with increasing heatup rates, each heatup rate must be analyzed on an individual basis.

Following the generation of pressure-temperature curves for both the steady-state and finite heatup rate situations, the final limit curves are produced by constructing a composite curve based on a point-by-point comparison of the steady-state and finite heatup rate data. At any given temperature, the allowable pressure is taken to be the lesser of the three values taken from the curves under consideration. The use of the composite curve is necessary to set conservative heatup limitations because it is possible for conditions to exist wherein, over the course of the heatup ramp, the controlling condition switches from the inside to the outside, and the pressure limit must at all times be based on analysis of the most critical criterion.

Finally, the 1983 Amendment to 10CFR50[A-4] has a rule which addresses the metal temperature of the closure head flange and vessel flange regions. This rule states that the metal temperature of the closure flange regions must exceed the material RT_{NDT} by at least 120°F for normal operation when the pressure exceeds 20 percent of the preservice hydrostatic test pressure.

Table A-1 indicates that the limiting RT_{NDT} of 40°F occurs in the closure head flange of McGuire Unit 1, so the minimum allowable temperature of this region is 160°F. These limits are less restrictive than the curves shown on figures A-2 and A-3.

A-4. HEATUP AND COOLDOWN LIMIT CURVES

Limit curves for normal heatup and cooldown of the primary Reactor Coolant System have been calculated using the methods discussed in section 3.0, and the procedure is presented in reference A-5. Figure A-2 is the heatup curve for 60°F/hr and applicable for the first 32 EFPY with margins for possible instrumentation errors. Figure A-3 is the cooldown curve up to 100°F/hr and applicable for the first 32 EFPY with margins for possible instrumentation errors.

Allowable combinations of temperature and pressure for specific temperature change rates are below and to the right of the limit lines shown in figures A-2 and A-3. This is in addition to other criteria which must be met before the reactor is made critical.

The leak limit curve shown in figure A-2 represents minimum temperature requirements at the leak test pressure specified by applicable codes[A-2,A-3]. The leak test limit curve was determined by methods of references A-2 and A-4.

Figures A-2 and A-3 define limits for ensuring prevention of nonductile failure for the McGuire Unit 1 Primary Reactor Coolant System.

A-5. ADJUSTED REFERENCE TEMPERATURE

From Regulatory Guide 1.99 Rev. 2 [A-1] the adjusted reference temperature (ART) for each material in the beltline is given by the following expression:

$$ART = \text{Initial } RT_{NDT} + \Delta RT_{NDT} + \text{Margin} \qquad (3)$$

Initial RT_{NDT} is the reference temperature for the unirradiated material as defined in paragraph NB-2331 of Section III of the ASME Boiler and Pressure Vessel Code. If measured values of initial RT_{NDT} for the material in question are not available, generic mean values for that class of material may be used if there are sufficient test results to establish a mean and standard deviation for the class.

ΔRT_{NDT} is the mean value of the adjustment in reference temperature caused by irradiation and should be calculated as follows:

$$\Delta RT_{NDT} = [CF]f^{(0.28-0.10 \log f)} \qquad (4)$$

To calculate ΔRT_{NDT} at any depth (e.g., at 1/4T or 3/4T), the following formula must first be used to attenuate the fluence at the specific depth.

$$f_{(\text{depth } X)} = f_{\text{surface}}^{(e^{-.24x})} \qquad (5)$$

where x (in inches) is the depth into the vessel wall measured from the vessel inner (wetted) surface. The resultant fluence is then put into equation (4) to calculate ΔRT_{NDT} at the specific depth.

CF (°F) is the chemistry factor, obtained from reference A-1. Beltline region materials of McGuire Unit 1 are considered for the limiting material. Limiting material is found to be the lower shell longitudinal weld located at the 30° azimuthal angle. The calculation of ART for the limiting material is shown in table A-2. This calculation was used to develop heatup and cooldown curves for McGuire Unit 1.

TABLE A-1

MCGUIRE UNIT 1 REACTOR VESSEL TOUGHNESS TABLE (Unirradiated)

Component	Material Code Number	Cu (%)	Ni (%)	T_{NDT} (°F)	RT_{NDT} (°F)
Closure head dome	B5086-1	0.11	0.48	20	37[c]
Closure head segments	B5087	0.11	0.62	10	10[c]
Closure head flange	B5002	--	0.75	40[c]	40[c]
Vessel Flange	B4701	--	0.73	29[c]	29[c]
Inlet nozzle	B5003-1	0.12	0.68	60[c]	60[c]
Inlet nozzle	B5003-2	0.10	0.71	60[c]	60[c]
Inlet nozzle	B5003-3	0.10	0.69	60[c]	60[c]
Inlet nozzle	B5003-4	0.10	0.69	60[c]	60[c]
Outlet nozzle	B5004-1	--	0.74	60[c]	60[c]
Outlet nozzle	B5004-2	--	0.74	60[c]	60[c]
Outlet nozzle	B5004-3	--	0.71	60[c]	60[c]
Outlet nozzle	B5004-4	--	0.79	60[c]	60[c]
Upper shell	B5453-2	0.14	0.58	10	15[c]
Upper shell	B5011-2	0.10	0.54	10	27[c]
Upper shell	B5011-3	0.13	0.56	0	0[c]
Intermediate shell	B5012-1	0.13	0.60	-30	34
Intermediate shell	B5012-2	0.13	0.62	0	0
Intermediate shell	B5012-3	0.10	0.66	-20	-13
Lower shell	B5013-1	0.14	0.56	-10	0
Lower shell	B5013-2	0.10	0.52	-10	30
Lower shell	B5013-3	0.10	0.55	0	15
Bottom head segment	B5458-1	0.14	0.60	-70	-26[c]
Bottom head segment	B5458-2	0.15	0.54	-30	-15[c]
Bottom head segment	B5458-3	0.13	0.56	-20	2[c]
Bottom head dome	B5085-1	0.13	0.53	0	10[c]
Intermediate shell longitudinal weld seams	M1.22[a]	0.21	0.88	-60	-50
Intermediate shell to lower shell weld	G1.39	0.05	<0.20	-70	-70
Lower shell longitudinal weld seam	M1.32	0.20	0.87	--	-56[d]
Lower shell longitudinal weld seam	M1.33[b]	0.21	0.68	--	-56[d]
Lower shell longitudinal weld seam	M1.34[b]	0.30	0.64	--	-56[d]

a. Used in reactor vessel surveillance weldment
b. Used in weld root region only
c. Estimated per U.S. NRC Standard Review Plan[A-2]
d. Generic mean values per Ref. A-1

TABLE A-2

CALCULATION OF ADJUSTED REFERENCE TEMPERATURES FOR LIMITING MCGUIRE UNIT 1 REACTOR VESSEL MATERIAL - LONGITUDINAL WELD (LOWER SHELL)

Parameter	Regulatory Guide 1.99 - Revision 2, 32 EFPY: 1/4 T	3/4 T
Chemistry Factor, CF (°F)	204.15	204.15
Fluence, f (10^{19} n/cm^2)(a)	.842	.305
Fluence Factor, ff	.952	.675

****

ΔRT_{NDT} = CF x ff (°F)	194.3	137.8
Initial RT_{NDT}, I (°F) (b)	-56	-56
Margin, M (°F) (c)	65.5	65.5

****

Revision 2 to Regulatory Guide 1.99

Adjusted Reference Temperature, ART = Initial RT_{NDT} + ΔRT_{NDT} + Margin	203.8	147.3

****

(a) Fluence, f, is based upon f_{surf} (10^{19} n/cm^2, E>1 Mev) = 1.4 at 32 EFPY. The McGuire Unit 1 reactor vessel wall thickness is 8.465 inches at the beltline region.

(b) The initial RT_{NDT} (I) value for the weld is a generic value.

(c) Margin is calculated as, $M = 2 [\sigma_1^{\ 2} + \sigma_\Delta^{\ 2}]^{0.5}$. The standard deviation for the initial RT_{NDT} margin term (σ_I) is assumed to be 17°F since the initial RT_{NDT} is a generic mean value. The standard deviation for ΔRT_{NDT}, ($\sigma\Delta$) is 28°F for the weld.

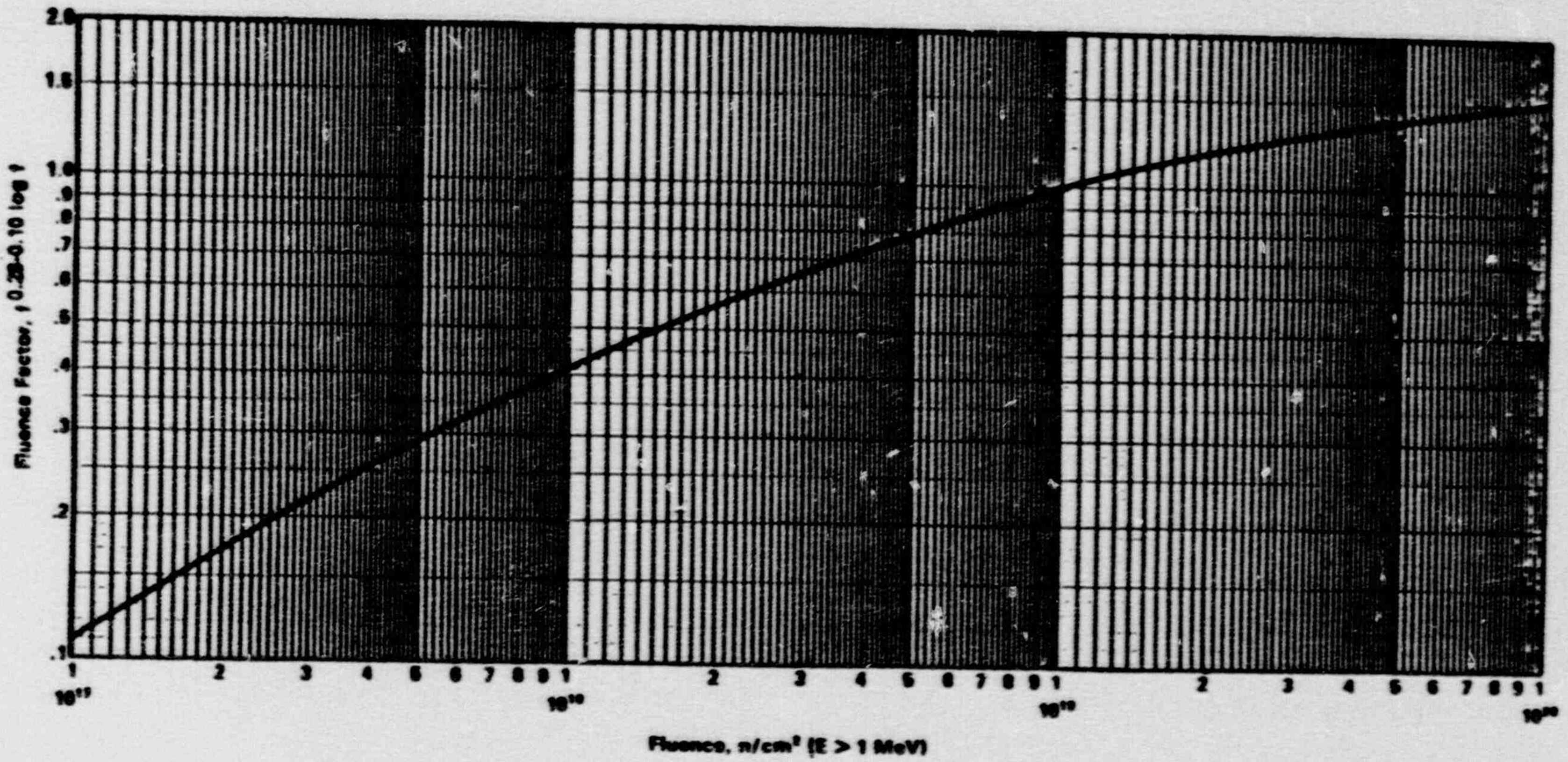

Figure A-1. Fluence Factor for Use in the Expression for ΔRT_{NDT}

3887s/082289:10

MATERIAL PROPERTY BASIS

CONTROLLING MATERIAL: LONGITUDINAL WELD

INITIAL RT_{NDT}: -56°F

RT_{NDT} AFTER 32 EFPY: 1/4T, 203.8°F

3/4T, 147.2°F

CURVES APPLICABLE FOR HEATUP RATES UP TO 60°F/HR FOR THE SERVICE PERIOD UP TO 32 EFPY. CONTAINS MARGIN OF 10°F AND 60 PSIG FOR POSSIBLE INSTRUMENT ERRORS.

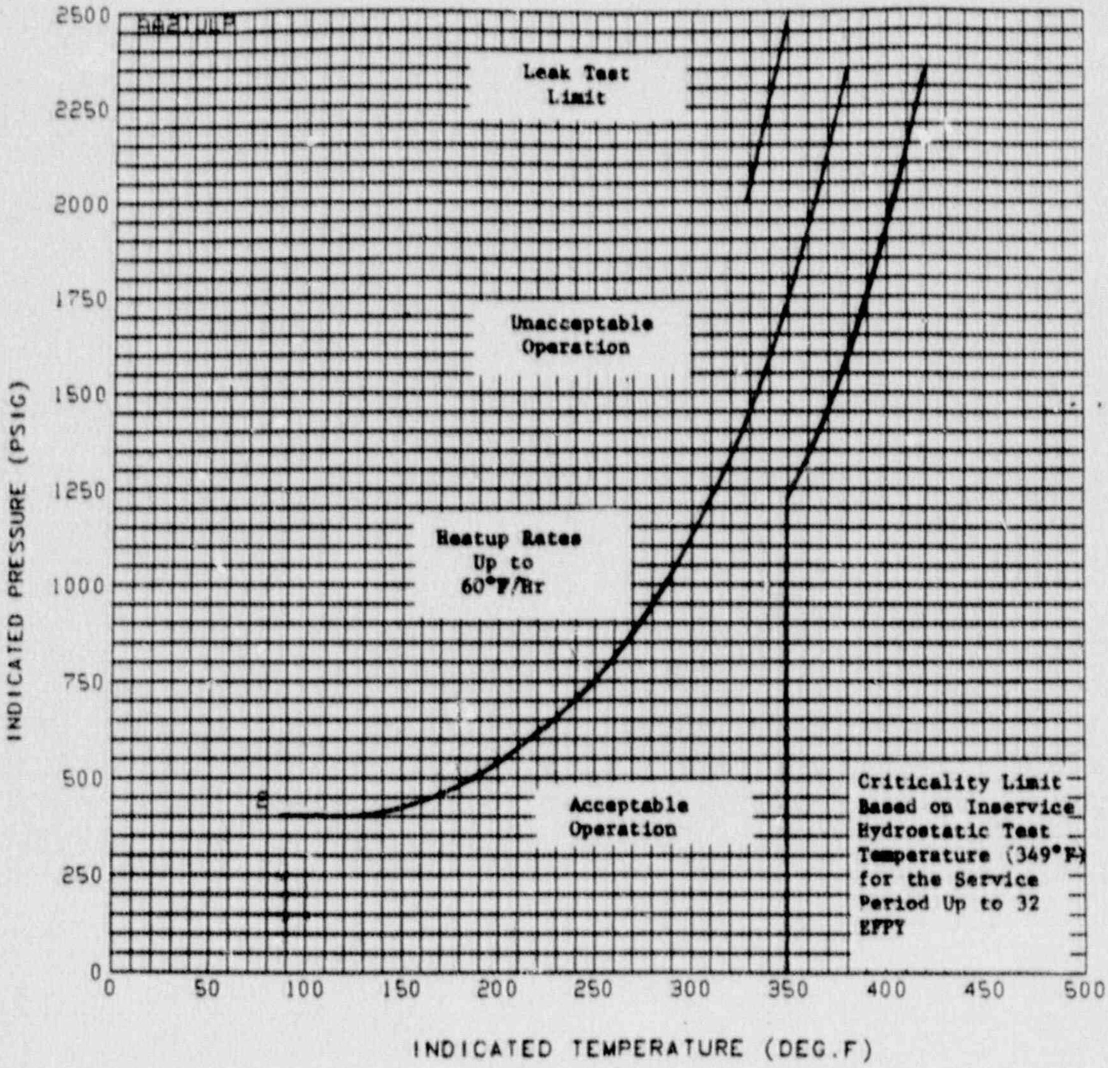

Figure A-2. McGuire Unit 1 Reactor Coolant System Heatup Limitations Applicable for the First 32 EFPY (With Margins For Instrumentation Errors)

MATERIAL PROPERTY BASIS

CONTROLLING MATERIAL: LONGITUDINAL WELD

INITIAL RT_{NDT}: -56°F

RT_{NDT} AFTER 32 EFPY: 1/4T, 203.8°F

3/4T, 147.2°F

CURVES APPLICABLE FOR COOLDOWN RATES UP TO 100°F/HR FOR THE SERVICE PERIOD UP TO 32 EFPY. CONTAINS MARGIN OF 10°F AND 60 PSIG FOR POSSIBLE INSTRUMENT ERRORS.

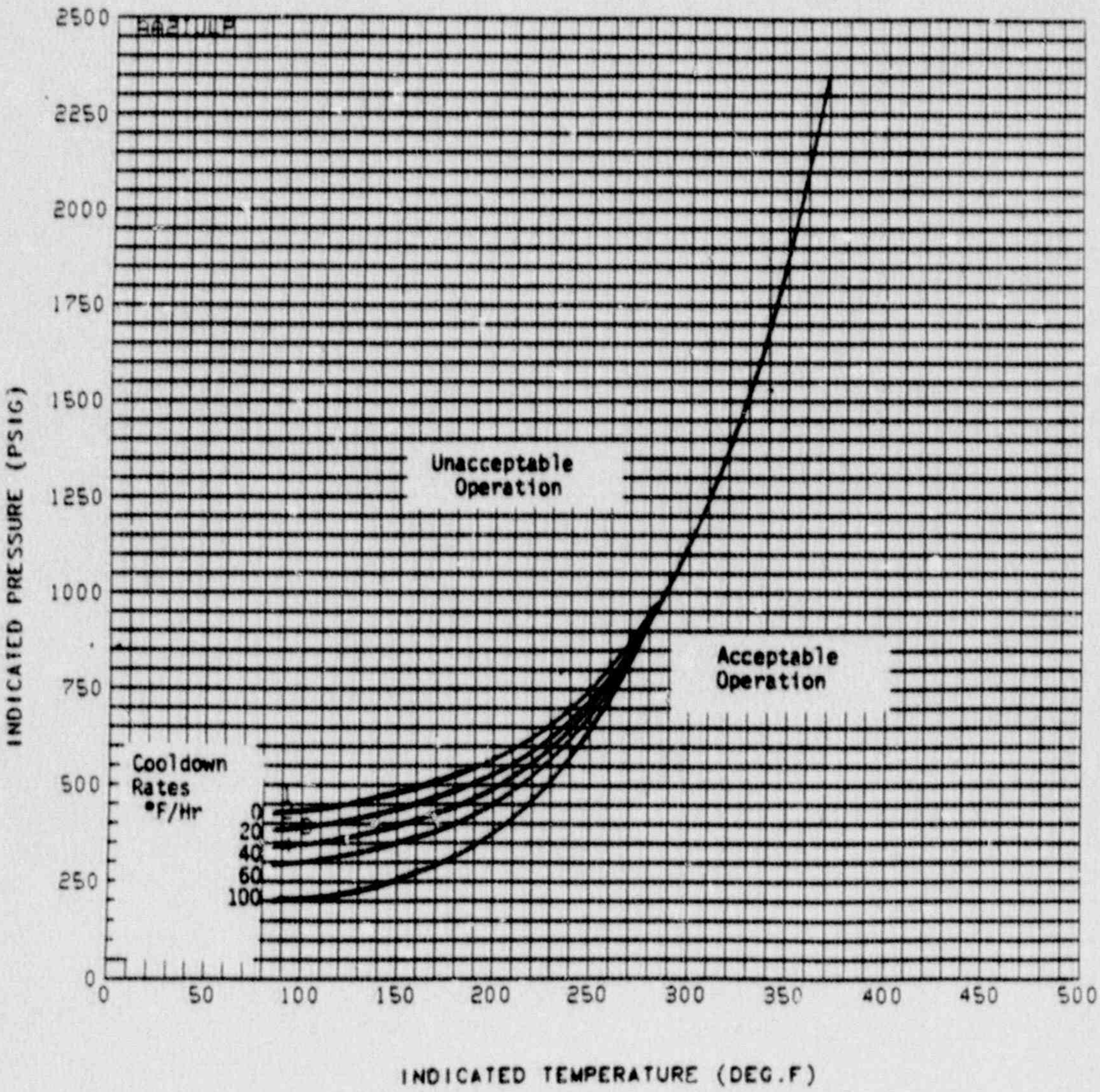

Figure A-3. Mcguire Unit 1 Reactor Coolant System Cooldown Limitations Applicable for the First 32 EFPY (With Margins For Instrumentation Errors)

A-7. REFERENCES

A-1 Regulatory Guide 1.99, Revision 2, "Radiation Embrittlement of Reactor Vessel Materials," U.S. Nuclear Regulatory Commission, May, 1988.

A-2 "Fracture Toughness Requirements," Branch Technical Position MTEB 5-2, Chapter 5.3.2 in Standard Review Plan for the Review of Safety Analysis Reports for Nuclear Power Plants, LWR Edition, NUREG-0800, 1981.

A-3 ASME Boiler and Pressure Vessel Code, Section III, Division 1 - Appendixes, "Rules for Construction of Nuclear Power Plant Components, Appendix G, Protection Against Nonductile Failure," pp. 558-563, 1986 Edition, American Society of Mechanical Engineers, New York, 1986.

A-4 Code of Federal Regulations, 10CFR50, Appendix G, "Fracture Toughness Requirements," U.S. Nuclear Regulatory Commission, Washington, D.C., Federal Register, Vol. 48 No. 104, May 27, 1983.

A-5 "Procedure for Developing Heatup and Cooldown Curves," Westinghouse Electric Corporation, Generation Technology Systems Division Procedure GTSD-A-1.12 (Rev. 0), July 13, 1988.

ATTACHMENT A

DATA POINTS FOR HEATUP AND COOLDOWN CURVES

(With Margins for Instrumentation Errors)

DAP COOLDOWN CURVES REG. GUIDE 1.99, REV. 2

08/18/89

THE FOLLOWING DATA WERE PLOTTED FOR COOLDOWN PROFILE 1 (STEADY-STATE COOLDOWN)

IRRADIATION PERIOD = 32.000 EFP YEARS
FLAW DEPTH = AOWIN T

	INDICATED TEMPERATURE (DEG.F)	INDICATED PRESSURE (PSI)		INDICATED TEMPERATURE (DEG.F)	INDICATED PRESSURE (PSI)		INDICATED TEMPERATURE (DEG.F)	INDICATED PRESSURE (PSI)
1	85.000	426.26	21	185.000	532.03	40	280.000	940.10
2	90.000	428.71	22	190.000	542.44	41	285.000	980.91
3	95.000	431.25	23	195.000	553.64	42	290.000	1024.78
4	100.000	434.08	24	200.000	565.66	43	295.000	1071.82
5	105.000	437.12	25	205.000	578.47	44	300.000	1122.37
6	110.000	440.39	26	210.000	592.39	45	305.000	1176.68
7	115.000	443.90	27	215.000	607.35	46	310.000	1234.73
8	120.000	447.68	28	220.000	623.26	47	315.000	1297.39
9	125.000	451.74	29	225.000	640.55	48	320.000	1364.53
10	130.000	456.11	30	230.000	659.12	49	325.000	1436.39
11	135.000	460.80	31	235.000	678.92	50	330.000	1513.31
12	140.000	465.85	32	240.000	700.38	51	335.000	1596.25
13	145.000	471.28	33	245.000	723.28	52	340.000	1684.86
14	150.000	477.01	34	250.000	748.08	53	345.000	1779.67
15	155.000	483.28	35	255.000	774.54	54	350.000	1881.21
16	160.000	490.02	36	260.000	803.14	55	355.000	1989.91
17	165.000	497.28	37	265.000	833.78	56	360.000	2106.07
18	170.000	505.07	38	270.000	866.62	57	365.000	2230.10
19	175.000	513.45	39	275.000	902.08	58	370.000	2362.43
20	180.000	522.45						

DAP COOLDOWN CURVES REG. GUIDE 1.99,REV.2

08/18/89

THE FOLLOWING DATA WERE PLOTTED FOR COOLDOWN PROFILE 2 (20 DEG-F / HR COOLDOWN)

IRRADIATION PERIOD = 32.000 EFP YEARS
FLAW DEPTH = AOWIN T

	INDICATED TEMPERATURE (DEG.F)	INDICATED PRESSURE (PSI)		INDICATED TEMPERATURE (DEG.F)	INDICATED PRESSURE (PSI)		INDICATED TEMPERATURE (DEG.F)	INDICATED PRESSURE (PSI)
1	85.000	382.81	16	160.000	448.35	30	230.000	627.60
2	90.000	385.22	17	165.000	455.95	31	235.000	648.97
3	95.000	387.85	18	170.000	464.12	32	240.000	671.74
4	100.000	390.67	19	175.000	472.95	33	245.000	696.48
5	105.000	393.74	20	180.000	482.32	34	250.000	722.85
6	110.000	397.03	21	185.000	492.56	35	255.000	751.43
7	115.000	400.61	22	190.000	503.55	36	260.000	782.01
8	120.000	404.45	23	195.000	515.42	37	265.000	814.86
9	125.000	408.62	24	200.000	528.04	38	270.000	850.38
10	130.000	413.10	25	205.000	541.79	39	275.000	888.42
11	135.000	417.95	26	210.000	556.57	40	280.000	929.31
12	140.000	423.16	27	215.000	572.36	41	285.000	973.30
13	145.000	428.79	28	220.000	589.48	42	290.000	1020.50
14	150.000	434.76	29	225.000	607.93	43	295.000	1071.26
15	155.000	441.31						

DAP COOLDOWN CURVES REG. GUIDE 1.99,REV.2

08/18/89

THE FOLLOWING DATA WERE PLOTTED FOR COOLDOWN PROFILE 3 (40 DEG-F / HR COOLDOWN)

IRRADIATION PERIOD = 32.000 EFP YEARS
FLAW DEPTH = AOWIN T

	INDICATED TEMPERATURE (DEG.F)	INDICATED PRESSURE (PSI)		INDICATED TEMPERATURE (DEG.F)	INDICATED PRESSURE (PSI)		INDICATED TEMPERATURE (DEG.F)	INDICATED PRESSURE (PSI)
1	85.000	338.46	15	155.000	398.59	29	225.000	575.53
2	90.000	340.84	16	160.000	405.97	30	230.000	596.75
3	95.000	343.47	17	165.000	413.96	31	235.000	619.49
4	100.000	346.25	18	170.000	422.56	32	240.000	644.11
5	105.000	349.35	19	175.000	4[illegible]1.79	33	245.000	670.48
6	110.000	352.70	20	180.000	441.81	34	250.000	699.03
7	115.000	356.38	21	185.000	452.65	35	255.000	729.60
8	120.000	360.28	22	190.000	464.31	36	260.000	762.45
9	125.000	364.57	23	195.000	476.80	37	265.000	798.07
10	130.000	369.18	24	200.000	490.36	38	270.000	836.20
11	135.000	374.21	25	205.000	505.01	39	275.000	877.22
12	140.000	379.54	26	210.000	520.75	40	280.000	921.30
13	145.000	385.41	27	215.000	537.64	41	285.000	968.77
14	150.000	391.73	28	220.000	555.93	42	290.000	1019.80

DAP COOLDOWN CURVES REG. GUIDE 1.99,REV.2

08/18/89

THE FOLLOWING DATA WERE PLOTTED FOR COOLDOWN PROFILE 4 (60 DEG-F / HR COOLDOWN)

IRRADIATION PERIOD = 32.000 EFP YEARS
FLAW DEPTH = ADWIN T

	INDICATED TEMPERATURE (DEG.F)	INDICATED PRESSURE (PSI)		INDICATED TEMPERATURE (DEG.F)	INDICATED PRESSURE (PSI)		INDICATED TEMPERATURE (DEG.F)	INDICATED PRESSURE (PSI)
1	85.000	282.80	15	155.000	355.07	29	225.000	543.73
2	90.000	295.26	16	160.000	362.84	30	230.000	566.51
3	95.000	287.83	17	165.000	371.28	31	235.000	590.98
4	100.000	300.79	18	170.000	380.30	32	240.000	617.43
5	105.000	303.89	19	175.000	390.16	33	245.000	645.87
6	110.000	307.30	20	180.000	400.79	34	250.000	676.43
7	115.000	311.05	21	185.000	412.30	35	255.000	709.54
8	120.000	315.09	22	190.000	424.71	36	260.000	745.09
9	125.000	319.52	23	195.000	438.05	37	265.000	783.33
10	130.000	324.31	24	200.000	452.51	38	270.000	824.47
11	135.000	329.53	25	205.000	468.15	39	275.000	868.80
12	140.000	335.16	26	210.000	484.89	40	280.000	916.48
13	145.000	341.30	27	215.000	503.09	41	285.000	967.85
14	150.000	347.87	28	220.000	522.68	42	290.000	1023.06

DAP COOLDOWN CURVES REG. GUIDE 1.99,REV.2

08/18/89

THE FOLLOWING DATA WERE PLOTTED FOR COOLDOWN PROFILE 5 (100 DEG-F/HR COOLDOWN)

IRRADIATION PERIOD = 32.000 EFP YEARS
FLAW DEPTH = AOWIN T

	INDICATED TEMPERATURE (DEG.F)	INDICATED PRESSURE (PSI)		INDICATED TEMPERATURE (DEG.F)	INDICATED PRESSURE (PSI)		INDICATED TEMPERATURE (DEG.F)	INDICATED PRESSURE (PSI)
1	85.000	198.10	15	155.000	265.60	29	225.000	482.24
2	90.000	200.51	16	160.000	274.32	30	230.000	508.73
3	95.000	203.23	17	165.000	283.83	31	235.000	537.25
4	100.000	206.19	18	170.000	294.12	32	240.000	568.11
5	105.000	209.50	19	175.000	305.27	33	245.000	601.34
6	110.000	213.10	20	180.000	317.37	34	250.000	637.11
7	115.000	217.10	21	185.000	330.51	35	255.000	675.72
8	120.000	221.45	22	190.000	344.65	36	260.000	717.30
9	125.000	226.22	23	195.000	360.06	37	265.000	762.16
10	130.000	231.43	24	200.000	376.69	38	270.000	810.46
11	135.000	237.17	25	205.000	394.64	39	275.000	862.55
12	140.000	243.38	26	210.000	414.09	40	280.000	918.61
13	145.000	250.19	27	215.000	435.06	41	285.000	978.99
14	150.000	257.57	28	220.000	457.77			

DAP 60F/HR HEATUP CURVE REG. GUIDE 1.99,REV.2

08/[illegible]/89

COMPOSITE CURVE PLOTTED FOR HEATUP PROFILE 2 HEATUP RATE(S) (DEG.F/HR) = 60.0

IRRADIATION PERIOD = 32.000 EFP YEARS
FLAW DEPTH = (1-AOWIN)T

	INDICATED TEMPERATURE (DEG.F)	INDICATED PRESSURE (PSI)		INDICATED TEMPERATURE (DEG.F)	INDICATED PRESSURE (PSI)		INDICATED TEMPERATURE (DEG.F)	INDICATED PRESSURE (PSI)
1	85.000	426.26	21	185.000	493.44	41	285.000	980.91
2	90.000	428.71	22	190.000	507.72	42	290.000	1024.78
3	95.000	423.22	23	195.000	523.08	43	295.000	1071.82
4	100.000	413.88	24	200.000	539.79	44	300.000	1122.37
5	105.000	407.42	25	205.000	557.85	45	305.000	1176.68
6	110.000	403.11	26	210.000	577.16	46	310.000	1223.75
7	115.000	400.87	27	215.000	598.15	47	315.000	1273.98
8	120.000	400.18	28	220.000	620.57	48	320.000	1327.70
9	125.000	401.05	29	225.000	640.55	49	325.000	1385.57
10	130.000	403.12	30	230.000	659.12	50	330.000	1447.47
11	135.000	406.45	31	235.000	678.92	51	335.000	1513.44
12	140.000	410.77	32	240.000	700.38	52	340.000	1584.61
13	145.000	416.18	33	245.000	723.28	53	345.000	1660.47
14	150.000	422.49	34	250.000	748.08	54	350.000	1741.83
15	155.000	429.79	35	255.000	774.54	55	355.000	1828.74
16	160.000	437.90	36	260.000	803.14	56	360.000	1921.76
17	165.000	447.07	37	265.000	833.78	57	365.000	2021.21
18	170.000	457.16	38	270.000	866.62	58	370.000	2127.41
19	175.000	468.27	39	275.000	902.08	59	375.000	2240.85
20	180.000	480.26	40	280.000	940.10	60	380.000	2361.62

DAP 60F/HR HEATUP CURVE REG. GUIDE 1.99,REV.2 08/18/89

THE FOLLOWING DATA WERE CALCULATEDFOR THE INSERVICE HYDROSTATIC LEAK TEST.

MINIMUM INSERVICE LEAK TEST TEMPERATURE (32.000 EFPY)

PRESSURE (PSI)	TEMPERATURE (DEG.F)
2000	329
2485	349

PRESSURE (PSI)	PRESSURE STRESS (PSI)	1.5 K1M (PSI SQ.RT.IN.)
2000	22165	92673
2485	27384	115553